CSIRO PUBLISHING

# Australian Journal of Physics

Volume 50, 1997
© CSIRO Australia 1997

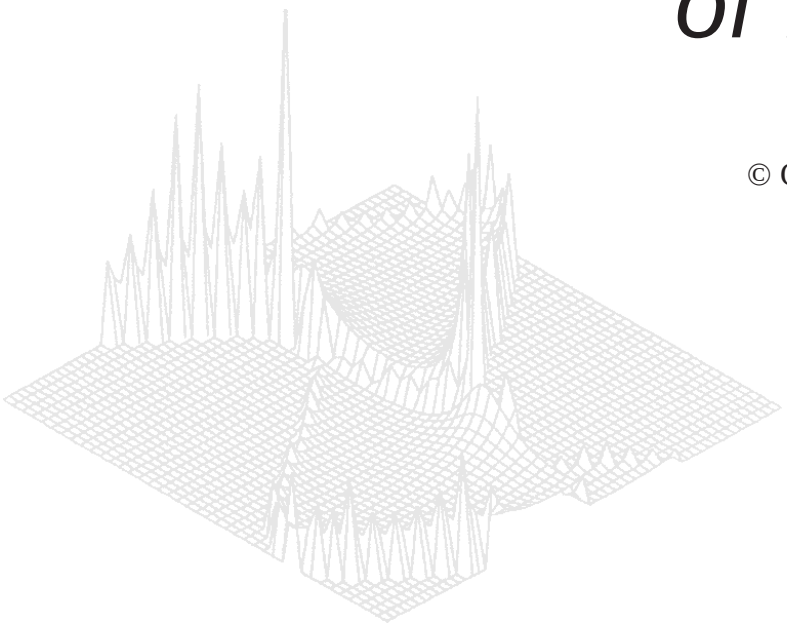

A journal for the publication of
original research in all branches of physics

**www.publish.csiro.au/journals/ajp**

All enquiries and manuscripts should be directed to
*Australian Journal of Physics*
**CSIRO** PUBLISHING
PO Box 1139 (150 Oxford St)
Collingwood Telephone: 61 3 9662 7626
Vic. 3066 Facsimile: 61 3 9662 7611
Australia Email: peter.robertson@publish.csiro.au

Published by **CSIRO** PUBLISHING
for CSIRO Australia and
the Australian Academy of Science

*Aust. J. Phys.*, 1997, **50**, 441–72

# Rotational and Vibrational Excitation of Nitrogen by Electron Impact*

*A. G. Robertson,*[A] *M. T. Elford,*[B] *R. W. Crompton,*[B]
*Michael A. Morrison,*[C] *Weiguo Sun*[D] *and W. K. Trail*[C]

[A] Department of Physics, University of Western Sydney, Nepean, Hawksbury Rd, Westmead, NSW 2145, Australia.
[B] Atomic and Molecular Physics Laboratories, Research School of Physical Sciences and Engineering, Australian National University, Canberra, ACT 0200, Australia.
[C] Department of Physics & Astronomy, University of Oklahoma, Norman, OK 73019–0225, USA.
[D] Department of Chemistry, Sichuan Union University, Chengdu, Sichuan 610065, People's Republic of China.

*Abstract*

Rotational excitation of nitrogen by low-energy electron impact has posed an unsolved problem for more than three decades. Early analysis of the results of swarm experiments in nitrogen found that the data could be matched remarkably well by assuming that the energy dependences of the $\Delta j = 2$ cross sections from threshold to a few tenths of an eV are given by a simple formula based on the Born approximation. Moreover, the quadrupole moment (the only adjustable parameter in the formula) which gave the best fit to the data was commensurate with existing experimental values. This finding posed an enigma, since the quadrupole Born expression is known to incorrectly represent the interaction potential for scattering except within a few meV of threshold. We have analysed new swarm data, taken in a dilute mixure of nitrogen in neon, using theoretical rotational and momentum transfer cross sections based on a solution of the Schrödinger equation using static, exchange, and polarisation potentials. This work explains the long-standing enigma and provides the basis for a subsequent analysis in which theoretical vibrational excitation cross sections are also investigated using the new swarm data for the mixture.

## 1. Introduction

There have been a number of theoretical studies of the rotational excitation of nitrogen by electron impact (see, for example, the papers cited by Huxley and Crompton 1974; Morrison *et al.* 1987*b*, 1996) but relatively few experimental tests of the cross sections. This situation stems from the very low thresholds (1·28 meV for the $j_0 = 0 \rightarrow j = 2$ transition, where $j$ is the rotational quantum number) and the close threshold spacings, which make crossed electron–molecule beam studies impractical. Nevertheless, what experimental evidence there is has revealed a curious anomaly which has never been satisfactorily explained—namely, that only the simplest theoretical description of the scattering process, the quadrupole Born theory of Gerjuoy and Stein (1955), which omits much of the essential physics, provides a satisfactory description of the results of swarm experiments when a

* Dedicated by his co-authors to Professor Robert W. Crompton on the occasion of his seventieth birthday.

10.1071/PH96092 0004-9506/97/030441$10.00

reasonable value of the molecular quadrupole moment is assumed. We review this background to the present work in Section 2.

Morrison *et al.* (1996) have recently reexamined this problem with the hope of explaining the paradox. Their treatment of ro–vibrational excitation, which is summarised in Section 3, includes polarisation, exchange, and correlation interactions and therefore approximates a complete picture of the scattering process. Their results show that competing interactions produce rotational cross sections that conform closely to the *form* of the quadrupole Born cross sections throughout the energy range that can be tested unambiguously by swarm experiments. This finding explains at least part of the paradox. However, there remains another serious problem: the cross sections that result from the new theory differ significantly in magnitude from those which are consistent with the available experimental transport data.

The principal aim of the new experimental work described in this paper was to discover the cause of this remaining disagreement between theory and experiment—in particular, whether it can be attributed to errors in the existing swarm data or their analysis. For reasons discussed later, we have chosen to measure and analyse drift velocities in a dilute mixture of nitrogen in a monatomic buffer gas, rather than drift velocities and diffusion coefficients in the pure gas. In neither approach is it possible to determine the cross sections for individual excitation processes because of the close threshold spacings and the large number of processes that have to be included in the analysis, even for gas temperatures as low as 77 K. Nevertheless, both approaches can be used to test cross sections determined theoretically, or by other experimental techniques, by comparing experimentally determined transport coefficients with values calculated using these cross sections.

In Section 4 we discuss possible sources of error in existing swarm data or its analysis, and explain why swarm experiments in an appropriate mixture were chosen for the present investigation. Section 5 describes the experiments themselves and their results. Section 6 uses the the new experimental results to examine the aforementioned problems regarding rotational excitation cross sections, while Section 7 extends the analysis to threshold vibrational excitation. We summarise in Section 8.

## 2. Background

Frost and Phelps (1962) were the first to make a detailed examination of rotational excitation by analysing electron transport coefficients measured in swarm experiments. Using their numerical solution of the Boltzmann equation they tested the validity of a set of cross sections generated by applying a formula derived some years earlier by Gerjuoy and Stein (1955). These authors assumed that rotational excitation of a diatomic molecule occurs solely through the long-range interaction of the incoming electron with the permanent quadrupole moment of the molecule, and therefore that the first Born approximation is applicable. Their quadrupole Born approximation (QBA) formula reads:

$$\sigma^{(r)}_{j_0 \to j_0+2}(E_0) = \frac{(j_0+2)(j_0+1)}{(2j_0+3)(2j_0+1)}\,\sigma_0\left[1-(4j_0+6)\frac{B_0}{E_0}\right], \qquad (1)$$

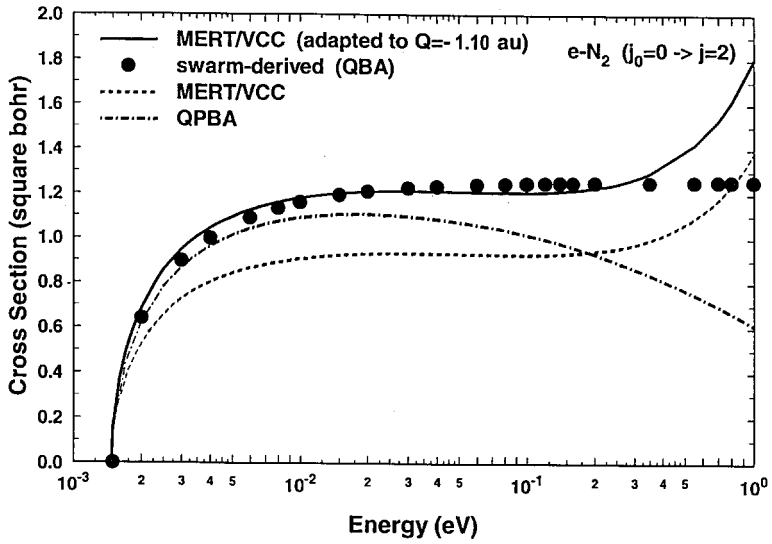


**Fig. 1.** Comparison of theoretical and experimental $j_0 = 0 \rightarrow j = 2$ cross sections. The QBA and QPBA cross sections were calculated using $Q = -1{\cdot}06\, ea_0^2$, the value found from swarm experiments (Haddad 1984). The MERT/VCC cross section of Morrison *et al.* (1996) is shown together with the cross section scaled by the factor $1{\cdot}30$ (see Section 6*a*).

where $E_0$ is the electron energy (in eV), $B_0$ is the rotational constant appropriate to the ground vibrational state ($2{\cdot}4805 \times 10^{-4}$ eV for $N_2$), $\sigma_0 = 8\pi\overline{Q}^2 a_0^2/15$, $\overline{Q}$ is the quadrupole moment averaged over the ground vibrational state, and $a_0$ is the Bohr radius. The $j_0 = 0 \rightarrow j = 2$ QBA swarm-derived cross section, as determined subsequently by Haddad (1984), see below, is shown in Fig. 1.

Frost and Phelps treated the quadrupole moment $\overline{Q}$ as an adjustable parameter and obtained the best fit to the available transport data with a value of $0{\cdot}95\, ea_0^2$. [In 1962, when they performed their analysis, there was doubt concerning the numerical value and sign of $\overline{Q}$. However, since $\sigma_0 \propto \overline{Q}^2$, the sign of $\overline{Q}$ does not affect the value of $\sigma^{(r)}_{j_0 \rightarrow j_0+2}(E_0)$ in equation (1). The presently accepted experimental value is $-1{\cdot}04 \pm 0{\cdot}07\, ea_0^2$, see Bridge and Buckingham (1966).]

Engelhardt *et al.* (1964) made a further analysis in the light of new developments in the theory of rotational excitation and additional experimental data. By then Dalgarno and Moffett (1963) and Mjolsness and Sampson (1964) had extended Gerjuoy and Stein's QBA theory by including a term in the interaction potential to account for the long-range induced polarisation interaction and had shown that at energies higher than a few millivolts above threshold these 'quadrupole-polarisation Born approximation' (QPBA) cross sections varied markedly from the QBA cross sections, lying well above or below them depending on whether $\overline{Q}$ was positive or negative. Fig. 1 illustrates the effect of including polarisation when, as is now known, $\overline{Q}$ is negative.

Engelhardt *et al.* drew the following surprising conclusions regarding the rotational cross sections: the best fit to the data was still that obtained by using the QBA cross sections (although with a value of $\overline{Q} = 1{\cdot}04\, ea_0^2$ which was somewhat higher than the value found by Frost and Phelps), and that the QPBA

cross sections 'led to less satisfactory agreement between theory and experiment than do the unmodified (i.e. QBA) cross sections', regardless of the sign of the value chosen for $\overline{Q}$.

Sampson and Mjolsness (1965) later treated the problem using the distorted wave approximation. The cross sections they obtained were much closer to the QBA cross sections than their earlier QPBA cross sections, the difference depending on the assumed value of $\overline{Q}$. In the case of the $j_0 = 4 \rightarrow j = 6$ cross section (the cross section for the rotational excitation that contributes most to the energy exchange at 77 K), the differences between the two cross sections were 6 and 10% at $0{\cdot}01$ and $0{\cdot}1$ eV respectively, with $\overline{Q} = -1{\cdot}04\, ea_0^2$.

Haddad (1984) reexamined the question of rotational excitation of nitrogen in his analysis of electron drift velocity data in argon–nitrogen mixtures. While his principal interest was in a more accurate determination of the normalising factor required to convert Schulz's (1964) relative vibrational excitation cross sections to absolute values, it was necessary to include rotational excitation in his analysis, as this was a significant energy loss process. He also assumed the QBA analytical form for these cross sections.

Haddad confirmed that the QBA cross sections provide the best fit to the transport data although he found that a slightly larger value of the quadrupole moment, $\overline{Q} = -1{\cdot}06\, ea_0^2$, gave the best overall agreement between the calculated and experimental results. This may in part have been due to the fact that he had access to additional data for $D_T/\mu$ (Crompton and Elford 1965, 1966—see Huxley and Crompton 1974) which were of somewhat higher accuracy than those available to Frost and Phelps and Engelhardt *et al.* A further analysis was made by Haddad and Phelps (1987) (see Crompton 1989) to test the compatibility with transport data of two new theoretical sets of rotational excitation cross sections, those of Onda (1985) and Morrison *et al.* (1987*b*). Both sets were found to be inconsistent with the available transport data.

The present work was motivated by the most recent work on low energy e–$N_2$ scattering by Morrison *et al.* (1996). As stated in the Introduction, the results of this work resolve the long-standing mystery of why only rotational cross sections of the QBA form have been able to reproduce measured transport data. This resolution, however, requires a modification to the magnitude of the quadrupole moment that results from the ab initio calculations, as discussed below. We now turn to the theory used to generate the cross sections used in the present analysis.

## 3. Theory

The theoretical cross sections for rotational excitation and momentum transfer used in the present analysis were generated using a two part procedure that entails numerical solution of vibrationally coupled scattering equations at energies above $0{\cdot}1$ eV and evaluation of simple analytic expressions based on modified effective range theory (MERT) below this energy. Both these methods have been described in detail in recent papers: the vibrational close coupling (VCC) calculations in Sun *et al.* (1995) and the use of MERT in Morrison *et al.* (1996). We also report new vibrational excitation cross sections calculated using the VCC method as detailed in Sun *et al.* (1995). In this section we recapitulate the high points of the theory in order to lay a foundation for the analysis and discussion of Sections 6 and 7.

*(3a) Vibrational Close Coupling*

The essential dynamical approximations underlying the present theoretical calculations of all cross sections at all energies are, first, that the molecule does not undergo electronic excitation and, second, that its rotational motion can be treated adiabatically. Both approximations are appropriate for electron induced elastic scattering and ro-vibrational excitation of $N_2$ at energies from a few hundredths of an eV to several eV (Lane 1980; Morrison 1988; Morrison *et al.* 1984*a*, 1984*b*).

We implement these assumptions as follows. First, we project out of the electron–molecule Schrödinger equation the (Born–Oppenheimer) ground electronic state wave function of the bound molecular electrons. Doing so precludes representation of correlation and polarisation effects via virtual electronic excitation; so we allow for these effects by adding to the e–$N_2$ interaction potential $V_{\rm int}$ an analytic correlation/polarisation term $V_{\rm c/p}$ described below.

Second, we 'freeze' the orientation of the internuclear axis in the solution of the scattering equations. This fixed nuclear orientation (FNO) approximation (Temkin and Vasavada 1967; Hara 1969) eliminates the rotational Hamiltonian from the Schrödinger equation; this operator can be recuperated asymptotically via a unitary transformation of the FNO scattering matrix. This transformation yields a $T$ matrix appropriate to rotational (or ro-vibrational) excitation in a space-fixed (laboratory) reference frame. If only vibrational excitation cross sections are required, this step can be bypassed, since the FNO scattering matrix directly yields a 'total' cross section for vibrational transitions $v_0 \to v$ (Lane 1980). Formally, this cross section equals the sum of ro-vibrational cross sections for all energetically allowed transitions $v_0 j_0 \to v j$:

$$\sigma^{(v)}_{v_0 \to v}(E_0) = \sum_{j=j_0}^{\infty} \sigma^{(rv)}_{v_0 j_0 \to v j}(E_0)\,. \tag{2}$$

In the FNO approximation, this sum is independent of the initial rotational quantum number $j_0$.

With this approximation, the projection on the internuclear axis $\hat{R}$ of the orbital angular momentum of the projectile $\ell$ is a good quantum number (Chang and Fano 1972). So solution of the Schrödinger equation is facilitated by writing it in a body fixed (BF) reference frame whose $z$ axis is coincident with the (fixed) internuclear axis $\hat{R}$. In such a formulation, scattering matrices are labelled by the channel labels $(v, \ell; \Lambda)$, where $v$ corresponds to the vibrational Hamiltonian. For a homonuclear target like $N_2$, the parity is also conserved, and we further label scattering matrices by $\eta$, as *gerade* $(\eta = g)$ or *ungerade* $(\eta = u)$.

In the body frame, we treat the vibrational dynamics by eigenfunction expansion (see Chang and Temkin 1969; Weatherford and Temkin 1994; Henry 1970; and the review by Morrison and Sun 1995). The first step in the reduction of the Schrödinger equation to a set of coupled radial scattering equations is to expand the wave function of the e–$N_2$ system in the complete set of reduced $N_2$ vibrational wave functions $\{\,\varphi_v(R)\,\}$. These we represent with Morse wave functions using the parameters $D_e = 0{\cdot}4480\,\text{Hartree}$, $\overline{\alpha}_M = 2{\cdot}5885\,a_0^{-1}$, and $R_e = 2{\cdot}02\,a_0$. These values reproduce the energies of the lowest 15 vibrational states of $N_2$ to four

decimal places (Huber and Herzberg 1979). The second step is expansion of the scattering functions in the complete set of spherical harmonics $\{ Y_\ell^\Lambda(\hat{r}) \}$. The full expansion of the BF-FNO system wave function is then

$$\psi^{\Lambda_\eta}_{v_0\ell_0}(\mathbf{r}, R) = \frac{1}{r} \sum_{v=0}^{v_{\max}} \sum_{\ell}^{\ell_{\max}} u^{\Lambda_\eta}_{v\ell,v_0\ell_0}(r) \varphi_v(R)\, Y_\ell^\Lambda(\hat{r})\,. \tag{3}$$

In practice both expansions are truncated at maximum quantum numbers, $v_{\max}$ and $\ell_{\max}$ respectively, chosen to ensure convergence of all reported scattering quantities to roughly 1%. The number of vibrational states $N_v$ and partial waves $N_\ell$ differs for resonant or non-resonant scattering and, in the latter case, depends on whether the energy is above or below the resonance region.

Substitution of this expansion into the Schrödinger equation leads to a set of coupled radial equations the solution of which leads, in turn, to the desired transition (T) matrix $\mathsf{T}^{\Lambda_\eta}$ with elements $T^{\Lambda_\eta}_{v\ell,v_0\ell_0}$. Since the wave function in the FNO approximation is independent of the sign of $\Lambda$, these equations separate into distinct sets identified by $|\Lambda| = 0, 1, \ldots$ (designated $\Sigma$, $\Pi$, $\ldots$) and—for homonuclear targets—by parity $\eta$. We thus solve for $T$ matrices that are characterised by symmetry classes $\Sigma_g$, $\Sigma_u$, $\Pi_u$, $\Pi_g$, etc. The corresponding partial cross sections are

$$\sigma^{\Lambda_\eta}_{v_0\to v}(E_0) \equiv \frac{\pi}{k_0^2} \sum_{\ell}^{\ell_{\max}} \sum_{\ell_0}^{\ell_{\max}} |T^{\Lambda_\eta}_{v\ell,v_0\ell_0}|^2\,. \tag{4}$$

The sum of these is the integral BF-FNO vibrational excitation cross section

$$\sigma_{v_0\to v}(E_0) = \sum_{\Lambda=0}^{\infty} \sum_{\eta} (2 - \delta_{\Lambda 0})\, \sigma^{\Lambda_\eta}_{v_0\to v}(E_0)\,. \tag{5}$$

The factor $(2 - \delta_{\Lambda,0})$ in (5) is required because for any value of $|\Lambda| > 0$, the orbital angular momentum projection quantum number can assume values $\pm\Lambda$.

In practice, we solve the scattering equations not for the $T$ matrix directly but rather for the reactance matrix $\mathsf{K}^{\Lambda_\eta}$, which corresponds to real boundary conditions. Once obtained, this $K$ matrix can be converted into a $T$ matrix via the transformation

$$\mathsf{T}^{\Lambda_\eta} = -2i\, \mathsf{K}^{\Lambda_\eta} \left(1 - i\, \mathsf{K}^{\Lambda_\eta}\right)^{-1}. \tag{6}$$

The factor $-2i$ corresponds to the convention $\mathsf{T}^{\Lambda_\eta} = 1 - \mathsf{S}^{\Lambda_\eta}$ (see the Appendix in Morrison and Sun 1995). We solve the (real) coupled radial equations using an integral equations algorithm (Sams and Kouri 1969; Morrison 1979; Morrison and Sun 1995). We first convert the radial differential equations to a set of coupled integral equations, then reduce this set to Volterra form. We solve the latter by numerical propagation from the origin to the asymptotic region.

*(3b) The e–$N_2$ Interaction Potential*

Low-energy vibrational excitation is acutely sensitive to all three constituents of the electron–molecule interaction potential (Lane 1980; Morrison 1983; Morrison *et al.* 1987*b*),

$$V_{\rm int}(\mathbf{r},R) = V_{\rm st}(\mathbf{r},R) + \hat{\mathcal{V}}_{\rm ex}(\mathbf{r},R) + V_{\rm c/p}(\mathbf{r},R)\,, \tag{7}$$

where $V_{\rm st}$ is the static (Coulomb) potential averaged over the ground electronic state of the target, $\hat{\mathcal{V}}_{\rm ex}$ is the bound–free exchange potential operator (whose non-local character is signified by the use of a script character), and $V_{\rm c/p}$ is the bound–free correlation/polarisation potential which incorporates at long range distortions of the target due to the projectile and at short range many body correlation effects (see Morrison 1979 and references therein). We calculate each constituent from an $R$-dependent near-Hartree–Fock (HF) wave function for the $X^1\Sigma_g^+$ Born–Oppenheimer ground electronic state of $N_2$. For this function we use the following grid of $R$ values (in $a_0$): $1{\cdot}60$, $1{\cdot}70$, $1{\cdot}80$, $1{\cdot}85$, $1{\cdot}90$, $1{\cdot}95$, $2{\cdot}00$, $2{\cdot}02$ $2{\cdot}068$, $2{\cdot}10$, $2{\cdot}20$, $2{\cdot}30$, $2{\cdot}40$, $2{\cdot}50$. From the large $r$ behaviour of the $\ell = 2$ projection of the static potential we can extract the $R$-dependent quadrupole moment. The average of this function $q(R)$ over the ground vibrational state yields $\langle\varphi_0 \mid q(R) \mid \varphi_0\rangle = -0{\cdot}961\, ea_0^2$, as compared to the experimental value $-1{\cdot}04 \pm 0{\cdot}07\, ea_0^2$ determined from measurements of induced birefringence (Bridge and Buckingham 1966). The implications of the slight difference between the experimental and theoretical quadrupole moments will be discussed in Section 6*b*.

For the exchange potential we use a model potential based on the extension by Hara (1967, 1969) to scattering problems of the familiar Slater average exchange potential for bound states. As implemented by Morrison and Collins (1978, 1982), this 'tuned free-electron–gas exchange' (TFEGE) potential is viable and accurate for vibrationally elastic scattering in the rigid-rotor approximation (Morrison and Collins 1978; Gibson and Morrison 1981) and for vibrational excitation of $H_2$ (Trail 1992; Morrison *et al.* 1984*a*).

For e–$N_2$ scattering the model exchange potential must be sufficiently flexible and robust to describe both resonant and non-resonant collisions at energies from a few tenths of an eV to several eV. This potential further must accommodate great differences in scattering in various electron–molecule symmetries. Many such symmetries contribute significantly to non-resonant elastic and inelastic cross sections, the importance of each depending on the scattering energy and excitation of interest. *Vibrationally inelastic* resonant e–$N_2$ cross sections, for example, are entirely determined by the $\Pi_g$ $T$ matrix (see Lane 1980 and references therein), while *vibrationally elastic* resonant cross sections entail significant contributions from both $\Pi_g$ and $\Sigma_g$ matrices.

Therefore, as detailed in Sun *et al.* (1995), we base our model exchange potential on separate $R$-dependent potentials for $\Sigma$ and $\Pi$ symmetries. Extensive tests showed that the resulting e–$N_2$ TFEGE potential accurately reproduces the complicated energy and $R$ dependencies of the resonant and non-resonant scattering matrices from 0 to 10 eV.

Finally, we come to the correlation/polarisation term $V_{\rm c/p}(\mathbf{r},R)$. Outside the charge cloud, this potential is determined as the difference between the mean

energies of the polarised and unpolarised systems. We generate these mean energies via the linear variational method, using our neutral $X^1\Sigma_g^+$ basis augmented with selected diffuse functions to allow sufficient flexibility for polarisation (Morrison *et al.* 1987*b*; Lane and Henry 1968; Gibson and Morrison 1984). One measure of the accuracy of this potential is the long-range (induced) moments of the target it predicts. The spherical and non-spherical polarisabilities $\overline{\alpha}_0(R)$ and $\overline{\alpha}_2(R)$, extracted from these moments at $r = 10\,a_0$, after averaging over the ground vibrational state, yield $\langle\varphi_0 \mid \overline{\alpha}_0 \mid \varphi_0\rangle = 10{\cdot}980\,a_0^3$ and $\langle\varphi_0 \mid \overline{\alpha}_2 \mid \varphi_0\rangle = 3{\cdot}096\,a_0^3$. The first value compares with the (room temperature) experimental spherical polarisability $11{\cdot}744 \pm 0{\cdot}004\,a_0^3$ measured by Newell and Baird (1965) and by Orcutt and Cole (1967). We can further assess this potential by comparing our non-spherical polarisabilities to estimates based on the relative polarisability anisotropy measured by Bridge and Buckingham (1966). For this estimate Miller and Bederson (1978) reported $3{\cdot}08 \pm 0{\cdot}002\,a_0^3$.

Inside the target charge cloud the correlation/polarisation potential is determined primarily by many-body effects arising from the correlation of the scattering electron and the bound electrons. This many-body phenomenon vitiates the independent particle model and yields a short-range non-local bound–free correlation potential. We approximate this potential using a parameter-free model first proposed by Temkin (1957) for electron–atom scattering. As discussed in detail elsewhere, we retain only the dipole term in the resulting model and so have named it the 'better-than-adiabatic-dipole' (BTAD) potential (Gibson and Morrison 1982, 1984; Morrison and Saha 1986; Morrison *et al.* 1987*b*; Morrison and Trail 1993).

### *(3c) Rotational Excitation at Very Low Energies*

In order to calculate momentum transfer and rotational excitation cross sections at energies below $0{\cdot}1$ eV without incurring the range of numerical problems that attend numerical solution of the Schrödinger equation at such energies, we have used a procedure that exploits the known analytic properties of the scattering matrix, as embodied in modified effective range theory (MERT), and approximate treatments of the rotational dynamics that ensure physically correct threshold behaviour of very low energy cross sections. In accordance with the MERT philosophy we extrapolate elements of the scattering matrix from energies above $0{\cdot}1$ eV, where they are (more or less) easily calculated from the Schrödinger equation, to lower energies. A detailed account of this approach together with demonstrations of its accuracy for e–$N_2$ scattering can be found in Morrison *et al.* (1996). In this present section we shall summarise the high points of this method and provide details required for the analysis of transport data that appears in the next section.

### *(3d) Extrapolation of Scattering Matrices to Very Low Energies*

Three theoretical assumptions underlie this procedure:

(1) At energies below about $0{\cdot}1$ eV, elements of the $S$ matrix corresponding to low partial wave order can be accurately approximated by analytic MERT expansions in powers of the exit channel electron wave number.
(2) $S$-matrix elements of high order can be approximated using the first Born approximation (FBA) (Morrison *et al.* 1984*a*; Isaacs and Morrison 1996),

since scattering in these channels is weak and accumulates over a very long range.

(3) We can approximate the rotational motion via an adiabatic approximation, augmented by a correction which ensures that elements of the scattering matrix depend correctly on energy near threshold.

The last of these assumptions is just the fixed nuclear orientation (FNO) approximation discussed above. In order to impose correct threshold behaviour on the resulting rotationally inelastic $T$-matrix elements, we apply the scaled adiabatic nuclear rotation theory of Feldt and Morrison (1984). Use of the Born approximation for high-order elements of the scattering matrix, now a standard approach in low-energy electron scattering calculations, is discussed at length in Morrison *et al.* (1984*a*) and in Isaacs and Morrison (1996).

Within this context, the way we calculate the reactance ($K$) matrix depends on whether the scattering energy is above or below a 'boundary energy' $E_{\mathrm{M}}$: for $E_0 \geq E_{\mathrm{M}}$, we solve the vibrational close coupling (VCC) radial equations using the static-exchange-polarisation potential described in the previous subsection and including the full complement of partial waves required to converge the scattering quantity of interest. The resulting matrix elements are used to determine the parameters for extrapolation to energies $E_0 \leq E_{\mathrm{M}}$. Expressions for $K$-matrix elements for electron scattering from a closed-shell non-polar molecule have been derived by Fabrikant (1984) and implemented for low-energy total e–$H_2$ and e–$N_2$ cross sections by Isaacs and Morrison (1992).

For use in the transport analysis reported here, we have calculated total momentum transfer $\sigma^{(m)}(E_0)$ and rotational excitation cross sections $\sigma^{(r)}_{j_0 \to j}(E_0)$. First, we generate $\sigma^{(m)}(E_0)$ from the $K$ matrix using equation (136) in Morrison and Sun (1995). This quantity is a *total* momentum transfer cross section; that is, it includes contributions from elastic scattering and rotational excitation for all open channels. Second, we calculate the rotational cross section from the $K$ matrix by first transforming this matrix into a $T$ matrix in a space-fixed laboratory frame whose $z$ axis is coincident with the incident electron wave vector $\mathbf{k}_0$. This transformation (Chang and Fano 1972) alters the representation of the $K$ matrix to that of lab-frame coupled angular momentum theory, in which channels are labelled $(v, j, \ell; J)$ with $J$ the total angular momentum of the system.

As noted above we further impose the requirement that all $T$-matrix elements which are important to the cross sections of interest go to zero properly at threshold. To this end we scale the frame transformed $T$-matrix elements by a ratio of matrix elements calculated in the first Born approximation (Feldt and Morrison 1984). This is the essence of the 'scaled adiabatic nuclear rotation' correction—see equations (140) and accompanying discussion in Morrison and Sun (1995); the required Born matrix elements can be found in the Appendix to Morrison *et al.* (1984*a*) and in Sec. III.A of Morrison and Sun (1995).

The theory described in this section was used to generate momentum transfer, rotational excitation, and vibrational excitation cross sections for the transport analysis in this paper. In order to emphasise the inelastic processes, the cross sections for which are of the greatest current interest, this analysis concerns swarm data not for pure $N_2$ but rather for a mixture of $N_2$ and Ne. The reasons for this choice are the subject of the next section.

## 4. The Method of Mixtures

The method of mixtures, as used by Haddad (1984), was adopted to make a sensitive and conclusive test of the new theoretical rotational and vibrational cross sections near threshold. This method, used first by Townsend and Bailey (1922) and subsequently by a number of workers (see, for example, Haddad and Crompton 1980; Haddad 1984; Petrović and Crompton 1987; England *et al.* 1988; England and Elford 1988, 1991; Schmidt *et al.* 1994), provides a means of either deriving more accurate elastic cross sections for the monatomic buffer gas or inelastic cross sections for the molecular additive (for a review see Schmidt 1995), or testing more definitively theoretically derived inelastic cross sections. Here we focus on the latter application as applied to the inelastic $N_2$ cross sections, and begin by briefly reviewing the method and its advantages.

In determining or testing a set of elastic and inelastic cross sections from transport data in a *pure* molecular gas, the analysis must be based on data for at least two transport coefficients and, unless the momentum transfer cross section is known, both it and the inelastic cross sections must be determined or tested simultaneously. The validity of the cross sections obtained from such analyses can then be queried on two grounds.

First, the determination from the Townsend–Huxley lateral diffusion experiment (Huxley and Crompton 1974) of one of the transport coefficients frequently used, namely the ratio of the lateral diffusion coefficient to the mobility $D_T/\mu$, involves the use of a semi-empirical relation, the so called 'Huxley ratio formula'. This formula is certainly valid in the 'asymptotic regime' (see Huxley and Crompton 1974), but it is not always possible to take measurements in this regime. While there is a considerable body of evidence to support the use of the formula outside this asymptotic regime, it has not been possible to substantiate its validity theoretically in circumstances where its application would seem to be questionable (England and Skullerud 1997; present issue p. 553).

The second problem is more fundamental and unavoidable, although its severity depends on the gas and the accuracy of the experimental data. It arises because there is an interaction between the influence of the momentum transfer and inelastic cross sections on the calculated transport coefficients, i.e. an error in an assumed set of inelastic cross sections can be partly compensated for by an adjustment to the momentum transfer cross section. While this effect is often of second order, it may nevertheless weaken the conclusions that can be drawn from tests based on an analysis of transport data in the pure molecular gas when both the momentum transfer and inelastic cross sections are unknown.

Both these problems can be avoided by measuring and analysing drift velocities in a gas mixture comprised of a monatomic buffer gas, for which the momentum transfer cross section is known, and a small fraction of molecular gas. The method relies on the possibility of finding a suitable buffer gas and mixture composition for which

- the aggregate momentum transfer cross section is dominated by that for the monatomic buffer gas;
- at a given value of $E/N$ (the ratio of electric field strength to gas number density), the energy exchange due to inelastic collisions with the molecular

component drastically changes the electron energy distribution function and hence the drift velocity from that for the pure buffer gas.

In this case, provided the momentum transfer cross section for the molecular gas is sufficiently well known that the uncertainty in its magnitude produces negligible uncertainty in the aggregate momentum transfer cross section for the mixture, the only unknowns in calculating the drift velocity for the mixture are the inelastic electron–molecule cross sections. Thus matching calculated and experimental drift velocity data alone is sufficient to determine these cross sections. In this way both the reliance on $D_T/\mu$ data and the 'cross talk' between the momentum transfer cross section and the inelastic cross sections inherent in analysing transport data for the pure molecular gas are eliminated.

The reason for the change in the drift velocity $v_{\rm dr}$ brought about by the addition of the molecular component can be seen from a simple formula that can be derived from momentum transfer theory (see, for example, Mason and McDaniel 1988), namely

$$v_{\rm dr} = \frac{eE}{m\langle\nu\rangle} = \frac{eE}{Nm\langle\sigma^{(m)}(E_0)\,v\rangle}\,, \tag{8}$$

where $\nu = N\sigma^{(m)}(E_0)\,v$ is the collision frequency for momentum transfer, and $v$ the electron speed. The average is taken over the distribution of electron speeds. The enhanced energy transfer due to the minor molecular constituent reduces the mean energy of the swarm, and thus, provided $\sigma^{(m)}$ for the mixture is nearly constant or increases with $v$, the drift velocity at a given $E/N$ is increased. Fig. 2 shows the large effect produced in the energy distribution function by the addition of $2{\cdot}1\%$ of $N_2$ to pure Ne at $E/N = 0{\cdot}01$ Td. (The correspondingly large increase in the drift velocity at that value of $E/N$ is shown in Fig. 5.)

Equation (8) also illustrates factors that determine the choice of buffer gas. First, the change in mean energy (and hence $v_{\rm dr}$) for a given fraction of the molecular additive will be greatest when the energy losses per collision with the atoms of the buffer gas are smallest, i.e. for the candidate gas with the largest atomic weight. Second, the effect of the additive will be enhanced if $\sigma^{(m)}$ increases with $v$ in the energy range of interest. In addition, the buffer gas with the largest momentum transfer cross section should be used in order to minimise the contribution from the molecular additive, and its cross section should be accurately known.

Neon was the best choice for the present investigation due to the convergence of the experimental and theoretical momentum transfer cross sections (Robertson 1972; O'Malley and Crompton 1980; Saha 1990; Gulley *et al.* 1994). It is superior to helium on the first two criteria, and only marginally inferior with respect to the accuracy with which the cross section is known. Argon has a larger atomic weight, and a larger cross section over much of the energy range of principal interest (0 to $0{\cdot}2$ eV), but the cross section decreases with energy in this range and is also subject to somewhat larger uncertainty.

## 5. Experimental Details

The drift velocities were measured by the Bradbury–Nielsen time-of-flight method using the technique and apparatus described by Huxley and Crompton

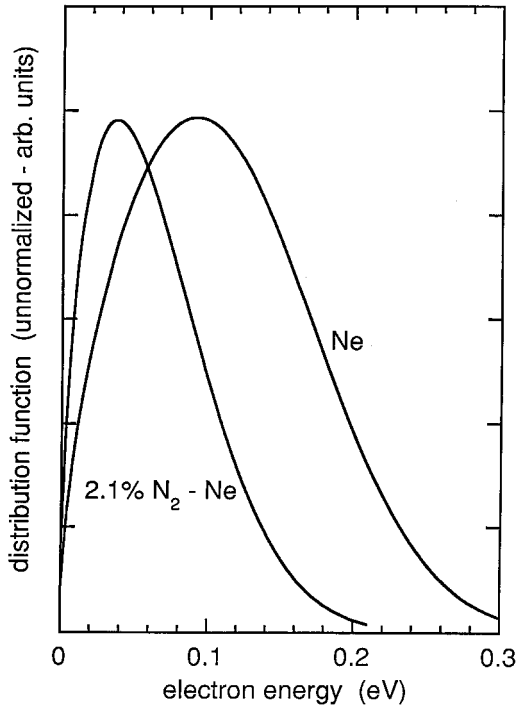


**Fig. 2.** Effect of the addition of 2·1% of $N_2$ to pure Ne (at $E/N = 0{\cdot}01$ Td) on the energy distribution function (unnormalised). (The corresponding effect on the drift velocity is shown in Fig. 5.)

(1974). Electrons were produced by $\alpha$-particle ionisation using an $Am^{241}$ foil as the particle source.

A gas temperature of 77 K was chosen for several reasons. First, electron swarms with very small mean energies are required to probe the rotational cross sections near threshold. The least energetic swarms possible are, of course, those in thermal equilibrium with the gas. At 77 K such swarms have a mean energy of about 10 meV, but a significant fraction of the electrons in them have energies less than 5 meV. But to approach this limit requires very small values of $E/N$ and hence values of $N$ larger than can be achieved at room temperature without exceeding atmospheric pressure. The higher gas densities achievable at 77 K is the second reason for doing the experiment at this temperature. Finally, the use of such a low gas temperature reduces the number of rotational levels with significant populations to about 12 and hence decreases the number of transitions that need to be taken into account. (At energies below about 1·25 eV, only $\Delta j = \pm 2$ transitions result in appreciable electron energy loss through rotational excitation.)

The drift length of the apparatus at 77 K was 9·980 cm. Gas pressures in the range 26 to 96 kPa (equivalent to a gas density of $9 \times 10^{19}$ cm$^{-3}$, or over 3·5 atmospheres at room temperature) were used in the experiments.

The optimum mixture concentration for this study is a compromise between several requirements:

- there must be sufficient $N_2$ in the mixture for the drift velocity to be adequately sensitive to the rotational (or vibrational) cross sections;
- the $N_2$ in the mixture must contribute only a small fraction to the aggregate $\sigma^{(m)}$ so the uncertainty in $\sigma^{(m)}$ for $N_2$ ($<\pm 5\%$, see below) has a negligible effect on the calculated drift velocities;
- at the lowest values of $E/N$ attainable in the measurements, the rate of energy transfer in the mixture must be such that a significant fraction of the electrons in the swarm has energies of only a few meV.

A series of preliminary computations indicated that a suitable compromise was a 2% $N_2$–98% Ne mixture.

The neon and nitrogen were Matheson Research Grade, used without further purification. The mixture was prepared by volume sharing using apparatus similar to that used by Haddad (1983). A period of five days then elapsed before measurements commenced to ensure complete mixing by diffusion. Due to experimental factors the mixture concentration differed slightly from the intended 2% $N_2$–98% Ne mixture and was $2{\cdot}085\%$ $N_2$–$97{\cdot}915\%$ Ne.

Pressures were measured using two calibrated quartz spiral manometers (Texas Instruments Ltd) which together covered the total pressure range to the required accuracy. Departures from the perfect gas law were taken into account when calculating the gas number density $N$ from the pressure.

Before beginning the drift velocity measurements in the mixture, we carried out a series of measurements in normal hydrogen at 293 K to check the operation of the drift tube and associated equipment. The measured drift velocities agreed with those obtained earlier by England *et al.* (1988) to within $0{\cdot}1\%$.

For the low temperature measurements in the mixture, the drift tube was immersed in a liquid nitrogen bath and the gas temperature taken to be the boiling point of the liquid ($76{\cdot}8$ K) after taking account of the level of impurity in it and the atmospheric pressure. A platinum resistance thermometer probe was used to detect any temperature variation due to contamination of the bath by dissolved oxygen. Copper-constantan thermocouples attached to the electrodes were used to check for any difference between the temperature of the electrode structure and the bath. The liquid nitrogen level was maintained constant to avoid significant pressure fluctuations.

All measurements were made using an automatic data acquisition system; a typical arrival time spectrum is shown in Fig. 3 which illustrates the level of precision with which the transit times can be determined. The drift velocity data in Table 1 show evidence of a small pressure dependence due to the effects of boundaries and other end effects (Huxley and Crompton 1974). The best estimate values of the drift velocity were obtained by extrapolation of plots of the measured drift velocity as a function of $1/p$ (where $p$ is the gas pressure) to $1/p = 0$. A typical such plot is shown in Fig. 4.

The final drift velocities are plotted in Fig. 5. The range of $E/N$ values used was $0{\cdot}0014$ to $0{\cdot}2$ Td, the lower limit being set by inadequate current for accurate measurement due to inadequate signal to noise and the upper limit by poor resolution of the arrival time spectra. The uncertainty of these results was

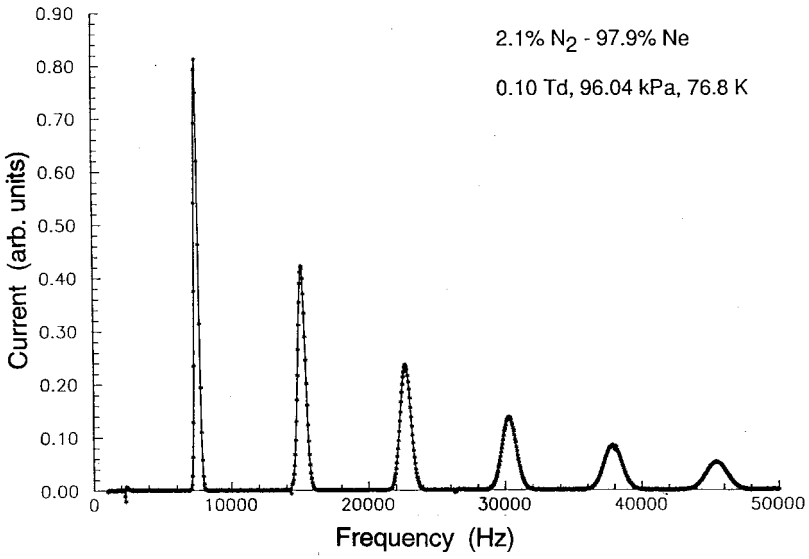


**Fig. 3.** Typical arrival time spectrum measured using the Bradbury–Nielsen time-of-flight method. The experimental conditions were 2·085% $N_2$–97·915% Ne mixture, 0·10 Td, 96·04 kPa and 76·8 K.

**Table 1. Measured electron drift velocities in a 2·085% $N_2$–97·915% Ne mixture at 76·8 K**
All entries are in $10^5$ cm s$^{-1}$. The top row shows pressures in kPa

| $E/N$ (Td) | 26·85 | 40·275 | 53·700 | 68·158 | 81·579 | 96·037 | Best est. |
|---|---|---|---|---|---|---|---|
| 0·0014 | | | | | | 0·868 | 0·86 |
| 0·0016 | | | | | | 0·938 | 0·93 |
| 0·0018 | | | | | 1·007 | 1·008 | 1·00 |
| 0·002 | | | | 1·074 | 1·069 | 1·068 | 1·052 |
| 0·003 | | | 1·284 | 1·282 | 1·279 | 1·277 | 1·269 |
| 0·004 | | | 1·391 | 1·390 | 1·388 | 1·386 | 1·380 |
| 0·005 | | 1·449 | 1·449 | 1·476 | 1·475 | 1·474 | 1·471 |
| 0·006 | | 1·479 | 1·479 | 1·476 | 1·475 | 1·474 | 1·471 |
| 0·007 | | 1·495 | 1·495 | 1·492 | 1·492 | 1·491 | 1·488 |
| 0·008 | | 1·510 | 1·504 | 1·502 | 1·501 | 1·500 | 1·493 |
| 0·009 | | 1·512 | 1·510 | 1·509 | 1·507 | 1·507 | 1·503 |
| 0·010 | 1·519 | 1·516 | 1·515 | 1·513 | 1·511 | 1·510 | 1·508 |
| 0·011 | 1·524 | 1·520 | 1·518 | 1·515 | 1·514 | 1·514 | 1·510 |
| 0·012 | 1·526 | 1·523 | 1·522 | 1·520 | 1·518 | 1·518 | 1·515 |
| 0·02 | 1·577 | 1·577 | 1·573 | 1·572 | 1·571 | 1·570 | 1·568 |
| 0·04 | 1·862 | 1·860 | 1·855 | 1·855 | 1·854 | 1·852 | 1·849 |
| 0·06 | 2·115 | 2·110 | 2·109 | 2·108 | 2·105 | 2·105 | 2·102 |
| 0·08 | 2·315 | 2·312 | 2·308 | 2·309 | 2·307 | 2·307 | 2·304 |
| 0·10 | 2·491 | 2·486 | 2·483 | 2·483 | | | 2·476 |
| 0·12 | 2·654 | 2·651 | 2·647 | | | | 2·642 |
| 0·14 | 2·818 | 2·815 | 2·810 | | | | 2·804 |
| 0·16 | 2·985 | 2·984 | | | | | 2·981 |
| 0·18 | 3·155 | 3·152 | | | | | 3·147 |
| 0·20 | 3·335 | 3·332 | | | | | 3·326 |

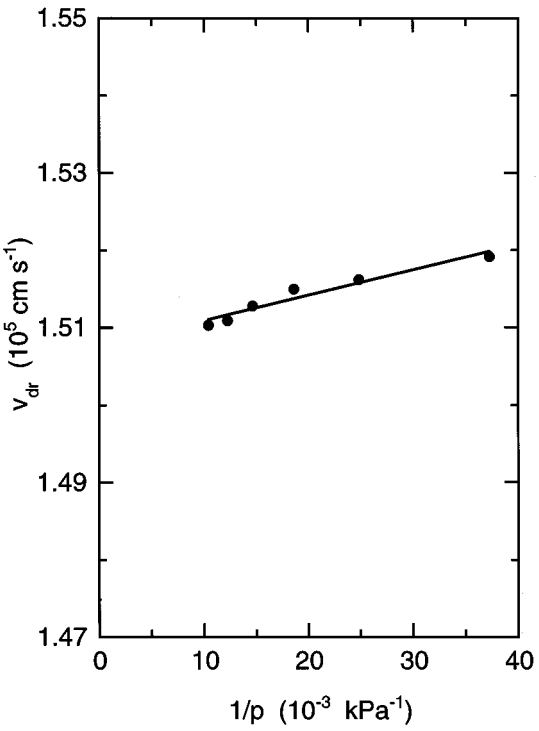


**Fig. 4.** Typical dependence of the measured drift velocity $v_{\rm dr}$ on $1/p$, indicating the statistical scatter and the uncertainty due to the extrapolation to $1/p = 0$. The experimental conditions were $0{\cdot}01$ Td and $76{\cdot}8$ K.

calculated by the method used by England *et al.* (1988) and is estimated to be $\pm 1\%$ for all the values of $E/N$ used.

## 6. Tests of Rotational Excitation Cross Sections

The first and principal application of the new drift velocity results in the mixture was to check the conclusion from previous swarm experiments that one must use QBA rotational cross sections in the low-energy region in order to reproduce measured transport coefficients. The success or failure of calculations using these QBA rotational cross sections to predict the new experimental data would either support or discount the caveats that were discussed in Section 4 with respect to the earlier swarm results. The second application was to test the QPBA cross sections in order to investigate the sensitivity of the new experimental data to the energy dependence of the rotational cross sections. The third and final application was to test these data against the MERT/VCC cross sections.

In each case the test comprised a comparison of experimental drift velocities with those calculated with the given set of cross sections. The drift velocities were calculated with the two-term Boltzmann code of Gibson (1970). A number of authors have shown that only in a very few special cases is the two-term code inadequate for calculating drift velocities, in which case a multi-term code must be used (see, for example, Haddad 1984; Petrović and Crompton 1987; England

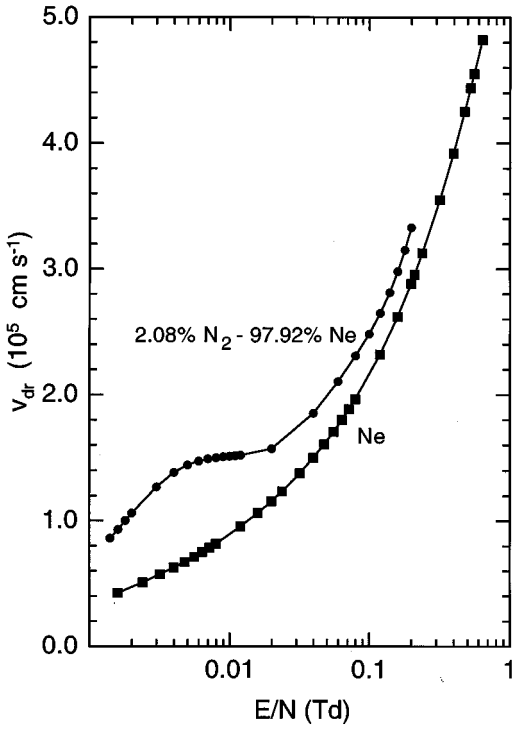


**Fig. 5.** 'Best estimate' values of the electron drift velocity in a 2·085% $N_2$–97·915% Ne mixture at 76·8 K. The values of the drift velocity in pure Ne at 76·8 K (Robertson 1972) are shown for comparison.

*et al.* 1988). We calculated the momentum transfer cross section for the mixture from the e–Ne cross section derived from Robertson's drift velocity data for pure neon (Robertson 1972; O'Malley and Crompton 1980) and the theoretical e–$N_2$ cross section of Morrison *et al.* (1996). At the low energies required for these tests (less than 0·25 eV) this e–$N_2$ cross section agrees to within 1% with that derived from swarm data by Engelhardt *et al.* (1964) and Haddad (1984) (see Fig. 6). As mentioned earlier, because of the small relative abundance of nitrogen present, the uncertainty in the $\sigma^{(m)}$ used for $N_2$ has a negligible effect on the calculated drift velocities. Nevertheless, for consistency we based the present analysis on MERT/VCC momentum transfer cross sections, as provided in a convenient analytic fit by Morrison *et al.* (1996).

The drift velocity data used for these tests were limited to values of $E/N \leq 0{\cdot}012$ Td in order to avoid any significant effect from vibrational excitation. The upper limit was checked by showing that at that limit the calculated drift velocities changed by less than 0·1% when the vibrational cross sections were set to zero. Fig. 2 shows why vibrational excitation has a negligible effect on the drift velocities at this (and lower) values of $E/N$: a negligible fraction of the electrons in the swarm have energies exceeding the $0 \rightarrow 1$ vibrational excitation threshold at 0·29 eV. This restriction of the $E/N$ range limits the energy range over which the rotational excitation cross sections can be tested to

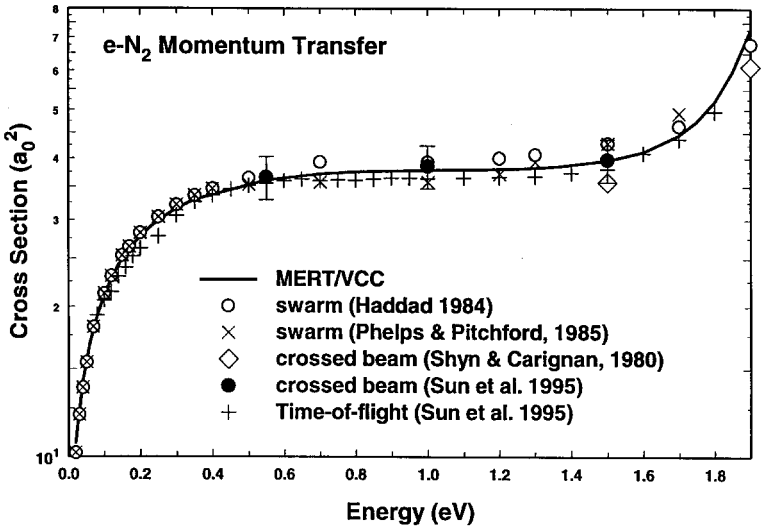


**Fig. 6.** Momentum transfer cross sections for e–$N_2$ scattering as calculated using the MERT/VCC theory of Morrison *et al.* (1996) (solid curve). Also shown are the swarm-derived cross sections of Haddad (1984) (open circles) and of Phelps and Pitchford (1985) (crosses), and a crossed-beam result by Shyn and Carignan (1980) (open diamonds). The crossed-beam results of Sun *et al.* (1995) (closed circles) were determined from measured angular distributions using the differential cross section extrapolation procedure discussed in Sun *et al.* (1995). Finally, the time-of-flight results (plusses) were determined by scaling time-of-flight total integral cross sections (Sun *et al.* 1995) by the ratio of theoretical VCC momentum transfer to integral cross sections (Buckman 1995).

less than about $0{\cdot}25$ eV, and therefore nothing significant can be inferred from the swarm data in this range of $E/N$ about the rapidly rising part of these cross sections at energies greater than $0{\cdot}2$ eV.

*(6a) Tests of the QBA and QPBA Cross Sections*

Fig. 7 shows the differences between the measured drift velocities and those calculated with the QBA and QPBA cross sections. Two observations can be made about these results:

(1) Since those calculated with the QBA cross sections (circles) agree to within experimental error with the measured drift velocities, no significant error in the cross sections derived from previous swarm experiments in pure nitrogen resulted either from the use of $D_T/\mu$ data from the Townsend–Huxley experiment or from lack of uniqueness in the analysis (see Section 4).

(2) The results calculated with the QPBA cross section (squares) indicate the sensitivity of the drift velocity data to the energy dependence of the rotational cross sections.

*(6b) Test of the MERT/VCC Cross Sections*

The differences that result when the drift velocities are calculated with the new theoretical cross sections (triangles) confirm the expectation that, although the cross sections have shapes close to the QBA cross sections (see Fig. 1), the differences in magnitude in the plateau region cause differences between calculated and experimental values of the drift velocity that lie well outside experimental error.

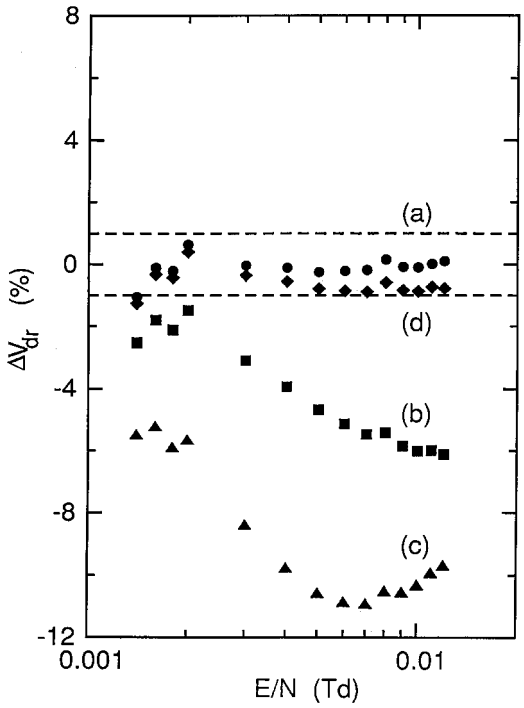


**Fig. 7.** The differences (%), as functions of $E/N$, between the measured drift velocities and those calculated for a 2·085% $N_2$–97·915% Ne mixture at 76·8 K, using the following sets of rotational excitation cross sections: (*a*) QBA (Gerjuoy and Stein 1955; Haddad 1984); (*b*) QPBA (Dalgarno and Moffett 1963, with the same value of $\overline{Q}$ as used in (*a*)); (*c*) MERT/VCC (Morrison *et al.* 1996); and (*d*) as for (*c*), multiplied by a factor of 1·3.

As detailed in Morrison *et al.* (1996), the agreement in shapes between the MERT/VCC and QBA cross sections is coincidental. Except very near threshold, the QBA does not accurately reflect the physics of rotational excitation, because it neglects all interactions except the long-range $r^{-3}$ static quadrupole term. Examination of key elements of the scattering matrices shows that at energies from slightly above threshold to several tenths of an eV, other interactions—the short- and intermediate-range static, exchange, polarisation interactions, and bound–free correlation—significantly affect rotational excitation. When these interactions are properly included and distortions of the scattering wave function from the free wave, which are neglected in the QBA (and QPBA) theories, are taken into account, the resulting cross sections exhibit an energy dependence quite akin to that of the QBA theory. *This coincidental resemblance between the shapes of the QBA and MERT/VCC rotational cross sections explains why in prior transport analysis of swarm data, only QBA rotational cross sections yielded transport coefficients that agreed with measured drift velocities.*

Having solved the paradox of the shape of the cross sections, we are left with the problem of why the MERT/VCC cross sections are too small to give calculated drift velocities that match the experimental data. In their paper

Morrison *et al.* (1996) show that the error in their rotational cross sections arises from the fact that their quadrupole moment, $\overline{Q} = -0{\cdot}961\, ea_0^2$, is somewhat smaller than the experimental value. This difference, in turn, arises from the use of a Hartree–Fock electronic wave function for the $X^1\Sigma_g$ ground electronic state of $N_2$. That is, the remaining error in the rotational cross section is a manifestation of the limitations of the Hartree–Fock approximation for the bound electrons. The effect of this limitation is most acute at very low energies, where $\sigma^{(r)}_{j_0 \to j_0+2}(E_0)$ is extremely sensitive to the value of $\overline{Q}$.

We can put this interpretation on a semi-quantitative basis and roughly assess the resulting error by noting that series expansion of the MERT rotational cross section (Fabrikant 1984) shows that the leading term from threshold to several tenths of an eV is proportional to $\overline{Q}^2$. So to crudely correct the MERT/VCC rotational cross sections we need only scale them by the square of the ratio of an empirical value of $\overline{Q}$ to the theoretical quadrupole moment. To bring the MERT/VCC cross sections close to the QBA cross sections for energies up to about $0{\cdot}3$ eV (see Fig. 1) and the calculated drift velocities for the mixture into agreement within experimental error (see Fig. 7, diamonds), we require a scaling factor of $1{\cdot}3$. This factor is equivalent to $\overline{Q} = 1{\cdot}1\, ea_0^2$. This quadrupole moment lies within the uncertainty of the experimental result of Bridge and Buckingham (1966), further confirming this interpretation of the source of the remaining difference between the QBA and MERT/VCC values. At higher energies, this argument is neither appropriate nor necessary; here the rotational cross sections rise rapidly as the influence of the $2{\cdot}8$ eV shape resonance grows as the energy moves into the resonance region from about $1{\cdot}5$ to $4{\cdot}0$ eV.

## 7. Extension to Near-threshold Vibrational Excitation

Although rotational excitation was the principal focus of the present work, the results from the drift velocity measurements in the mixture extended to sufficiently high values of $E/N$ that some assessment was possible of the VCC results for the $v_0 = 0 \to v = 1$ vibrational excitation cross section from threshold ($0{\cdot}288$ eV) to about 1 eV. In this energy range the cross section is determined almost entirely by direct excitation.

Theoretical VCC cross sections for the $0 \to 1$ vibrational excitation appear in Table 3. (The vibrationally elastic cross sections are shown in Table 2, and those for momentum transfer in Table 4.)* These data at energies below the resonance region are compared to experiment in Fig. 8*a*. Complementing this figure is the comparison in the resonance region in Fig. 8*b*. We now turn to a discussion of the implications of these cross sections for the present transport analysis.

Below the onset of the 2 eV resonance the cross section is small but finite, as first demonstrated experimentally by Engelhardt *et al.* (1964). Chen (1964) had earlier calculated the magnitude of the non-resonant cross section near threshold and found it to vary from about 3 to $6 \times 10^{-3}$ Å$^2$ over the energy range $0{\cdot}4$ to $1{\cdot}2$ eV. Engelhardt *et al.* found that it was not possible to obtain a satisfactory fit to the swarm data without including this so-called 'threshold foot' to the

* The cross sections in these tables are available on disc by request from Michael A. Morrison, Department of Physics & Astronomy, University of Oklahoma, Norman, OK 73019–0225, USA or by email from MORRISON@PHYAST.NHN.UOKNOR.EDU.

**Table 2. Theoretical MERT/VCC vibrationally elastic cross sections (in $a_0^2$) at selected energies**

The first four columns show partial cross sections; the last their sum. Note that Π partial cross sections have been multiplied by 2, as prescribed in equation (5)

| $E$ (eV) | $\Sigma_g$ | $\Sigma_u$ | $\Pi_u$ | $\Pi_g$ | Total |
|---|---|---|---|---|---|
| 0·020 | 8·118 | 0·162 | 0·742 | 0·010 | 9·037 |
| 0·040 | 10·750 | 0·099 | 0·925 | 0·007 | 11·790 |
| 0·060 | 12·750 | 0·067 | 1·111 | 0·007 | 13·950 |
| 0·080 | 14·430 | 0·049 | 1·230 | 0·007 | 15·730 |
| 0·100 | 15·870 | 0·038 | 1·323 | 0·007 | 17·270 |
| 0·120 | 17·140 | 0·030 | 1·397 | 0·008 | 18·610 |
| 0·140 | 18·280 | 0·025 | 1·455 | 0·010 | 19·810 |
| 0·160 | 19·310 | 0·022 | 1·500 | 0·012 | 20·890 |
| 0·180 | 20·250 | 0·020 | 1·535 | 0·014 | 21·870 |
| 0·200 | 21·120 | 0·018 | 1·560 | 0·016 | 22·770 |
| 0·230 | 22·300 | 0·017 | 1·583 | 0·020 | 23·980 |
| 0·260 | 23·350 | 0·017 | 1·591 | 0·025 | 25·060 |
| 0·290 | 24·310 | 0·017 | 1·588 | 0·030 | 26·020 |
| 0·320 | 25·180 | 0·017 | 1·575 | 0·036 | 26·890 |
| 0·350 | 25·970 | 0·019 | 1·554 | 0·043 | 27·680 |
| 0·550 | 29·910 | 0·045 | 1·295 | 0·108 | 31·500 |
| 0·700 | 31·830 | 0·092 | 1·048 | 0·192 | 33·350 |
| 0·800 | 32·800 | 0·137 | 0·884 | 0·273 | 34·300 |
| 1·000 | 34·180 | 0·264 | 0·589 | 0·534 | 35·830 |
| 1·250 | 35·210 | 0·486 | 0·306 | 1·224 | 37·550 |
| 1·330 | 35·410 | 0·571 | 0·237 | 1·611 | 38·180 |
| 1·361 | 35·480 | 0·604 | 0·213 | 1·794 | 38·450 |
| 1·500 | 35·700 | 0·768 | 0·126 | 3·018 | 40·010 |
| 1·600 | 35·790 | 0·895 | 0·081 | 4·539 | 41·720 |
| 1·700 | 35·830 | 1·028 | 0·051 | 7·199 | 44·550 |
| 1·750 | 35·830 | 1·097 | 0·042 | 9·338 | 46·770 |
| 1·800 | 35·830 | 1·167 | 0·035 | 12·430 | 49·940 |
| 1·850 | 35·810 | 1·239 | 0·032 | 16·990 | 54·560 |
| 1·860 | 35·810 | 1·253 | 0·032 | 18·110 | 55·690 |
| 1·900 | 35·790 | 1·312 | 0·032 | 22·860 | 60·490 |
| 1·950 | 35·750 | 1·386 | 0·035 | 24·070 | 61·750 |
| 1·980 | 35·730 | 1·430 | 0·038 | 18·280 | 56·000 |
| 2·000 | 35·710 | 1·461 | 0·041 | 13·780 | 51·520 |
| 2·040 | 35·680 | 1·521 | 0·048 | 9·978 | 47·760 |
| 2·050 | 35·670 | 1·537 | 0·049 | 10·240 | 48·030 |
| 2·067 | 35·650 | 1·563 | 0·053 | 11·590 | 49·400 |
| 2·084 | 35·630 | 1·589 | 0·057 | 13·940 | 51·770 |
| 2·100 | 35·610 | 1·613 | 0·061 | 16·990 | 54·830 |
| 2·160 | 35·540 | 1·707 | 0·077 | 35·500 | 73·390 |
| 2·200 | 35·490 | 1·770 | 0·091 | 50·070 | 88·000 |
| 2·300 | 35·340 | 1·928 | 0·130 | 20·500 | 58·500 |
| 2·350 | 35·260 | 2·009 | 0·153 | 12·100 | 50·140 |
| 2·400 | 35·170 | 2·089 | 0·177 | 23·110 | 61·180 |
| 2·410 | 35·150 | 2·106 | 0·183 | 27·610 | 65·680 |

**Table 2. Theoretical vibrationally elastic cross sections (in $a_0^2$)—continued**

| $E$ (eV) | $\Sigma_g$ | $\Sigma_u$ | $\Pi_u$ | $\Pi_g$ | Total |
|---|---|---|---|---|---|
| 2·415 | 35·140 | 2·114 | 0·185 | 30·120 | 68·200 |
| 2·420 | 35·140 | 2·122 | 0·188 | 32·770 | 70·850 |
| 2·423 | 35·130 | 2·127 | 0·190 | 34·420 | 72·510 |
| 2·425 | 35·130 | 2·130 | 0·191 | 35·550 | 73·630 |
| 2·430 | 35·120 | 2·138 | 0·193 | 38·400 | 76·490 |
| 2·450 | 35·080 | 2·171 | 0·204 | 49·530 | 87·630 |
| 2·460 | 35·060 | 2·187 | 0·210 | 53·910 | 92·020 |
| 2·467 | 35·050 | 2·198 | 0·214 | 56·070 | 94·180 |
| 2·484 | 35·020 | 2·226 | 0·224 | 57·240 | 95·360 |
| 2·487 | 35·010 | 2·231 | 0·225 | 56·830 | 94·950 |
| 2·490 | 35·010 | 2·236 | 0·227 | 56·240 | 94·360 |
| 2·494 | 35·000 | 2·242 | 0·229 | 55·190 | 93·320 |
| 2·495 | 35·000 | 2·244 | 0·230 | 54·890 | 93·010 |
| 2·500 | 34·990 | 2·252 | 0·233 | 53·140 | 91·270 |
| 2·600 | 34·790 | 2·416 | 0·296 | 15·130 | 53·310 |
| 2·700 | 34·570 | 2·581 | 0·365 | 34·690 | 72·920 |
| 2·733 | 34·500 | 2·636 | 0·389 | 44·190 | 82·430 |
| 2·766 | 34·430 | 2·691 | 0·413 | 45·030 | 83·280 |
| 2·770 | 34·420 | 2·697 | 0·417 | 44·550 | 82·810 |
| 2·800 | 34·350 | 2·747 | 0·440 | 38·700 | 76·970 |
| 2·850 | 34·230 | 2·830 | 0·479 | 26·850 | 65·140 |
| 2·860 | 34·210 | 2·846 | 0·487 | 24·830 | 63·120 |
| 2·900 | 34·110 | 2·913 | 0·520 | 18·800 | 57·110 |
| 2·925 | 34·050 | 2·954 | 0·540 | 16·980 | 55·300 |
| 2·950 | 33·990 | 2·996 | 0·562 | 16·850 | 55·180 |
| 3·000 | 33·870 | 3·078 | 0·604 | 21·450 | 59·790 |
| 3·033 | 33·790 | 3·133 | 0·633 | 26·110 | 64·470 |
| 3·066 | 33·710 | 3·187 | 0·663 | 29·310 | 67·670 |
| 3·100 | 33·620 | 3·244 | 0·694 | 29·780 | 68·150 |
| 3·115 | 33·580 | 3·268 | 0·707 | 29·190 | 67·560 |
| 3·200 | 33·360 | 3·408 | 0·786 | 22·230 | 60·630 |
| 3·250 | 33·230 | 3·490 | 0·834 | 18·610 | 57·020 |
| 3·300 | 33·100 | 3·572 | 0·883 | 16·940 | 55·360 |
| 3·340 | 32·990 | 3·637 | 0·922 | 17·260 | 55·690 |
| 3·350 | 32·970 | 3·653 | 0·932 | 17·520 | 55·950 |
| 3·400 | 32·830 | 3·735 | 0·982 | 18·990 | 57·430 |
| 3·420 | 32·780 | 3·767 | 1·002 | 19·360 | 57·800 |
| 3·450 | 32·690 | 3·816 | 1·032 | 19·480 | 57·930 |
| 3·500 | 32·560 | 3·896 | 1·084 | 18·650 | 57·110 |
| 3·600 | 32·280 | 4·056 | 1·188 | 15·610 | 54·080 |
| 3·700 | 32·000 | 4·214 | 1·294 | 13·960 | 52·440 |
| 3·800 | 31·720 | 4·371 | 1·401 | 14·070 | 52·560 |
| 3·900 | 31·440 | 4·526 | 1·510 | 13·580 | 52·080 |
| 4·000 | 31·150 | 4·679 | 1·621 | 12·470 | 50·970 |
| 4·500 | 29·720 | 5·412 | 2·183 | 9·365 | 47·860 |
| 5·000 | 28·300 | 6·086 | 2·747 | 7·794 | 46·230 |
| 6·000 | 25·580 | 7·250 | 3·833 | 6·133 | 44·360 |
| 7·000 | 23·090 | 8·172 | 4·819 | 5·416 | 43·310 |
| 8·000 | 20·860 | 8·878 | 5·685 | 5·051 | 42·530 |
| 9·000 | 18·890 | 9·400 | 6·434 | 4·850 | 41·860 |
| 10·0000 | 17·150 | 9·770 | 7·074 | 4·734 | 41·25 |

**Table 3. Theoretical MERT/VCC vibrationally inelastic 0 → 1 cross sections (in $a_0^2$) at selected energies**

The first four columns show partial cross sections; the last their sum. Note that Π partial cross sections have been multiplied by 2. Notation: $1{\cdot}0(-3) = 1 \times 10^{-3}$

| $E$ (eV) | $\Sigma_g$ | $\Sigma_u$ | $\Pi_u$ | $\Pi_g$ | Total |
|---|---|---|---|---|---|
| 0·290 | 1·019(−3) | 9·520(−5) | 1·815(−4) | 0·0001 | 0·0015 |
| 0·320 | 3·846(−3) | 9·687(−5) | 2·152(−4) | 0·0001 | 0·0044 |
| 0·350 | 4·577(−3) | 1·005(−4) | 2·767(−4) | 0·0001 | 0·0052 |
| 0·550 | 4·378(−3) | 1·463(−4) | 1·055(−3) | 0·0002 | 0·0060 |
| 0·700 | 3·653(−3) | 1·883(−4) | 1·871(−3) | 0·0005 | 0·0066 |
| 0·800 | 3·250(−3) | 2·168(−4) | 2·463(−3) | 0·0012 | 0·0075 |
| 1·000 | 2·635(−3) | 2·732(−4) | 3·672(−3) | 0·0054 | 0·0125 |
| 1·250 | 2·120(−3) | 3·411(−4) | 5·111(−3) | 0·0310 | 0·0391 |
| 1·330 | 1·996(−3) | 3·619(−4) | 5·539(−3) | 0·0537 | 0·0622 |
| 1·361 | 1·953(−3) | 3·697(−4) | 5·697(−3) | 0·0664 | 0·0750 |
| 1·500 | 1·780(−3) | 4·042(−4) | 6·386(−3) | 0·1833 | 0·1925 |
| 1·600 | 1·676(−3) | 4·277(−4) | 6·842(−3) | 0·4004 | 0·4100 |
| 1·700 | 1·587(−3) | 4·499(−4) | 7·268(−3) | 0·9632 | 0·9732 |
| 1·750 | 1·547(−3) | 4·605(−4) | 7·470(−3) | 1·5820 | 1·5920 |
| 1·800 | 1·510(−3) | 4·707(−4) | 7·664(−3) | 2·7450 | 2·7550 |
| 1·850 | 1·475(−3) | 4·805(−4) | 7·850(−3) | 5·0950 | 5·1060 |
| 1·860 | 1·469(−3) | 4·825(−4) | 7·887(−3) | 5·8110 | 5·8220 |
| 1·900 | 1·443(−3) | 4·900(−4) | 8·030(−3) | 9·8950 | 9·9060 |
| 1·950 | 1·414(−3) | 4·990(−4) | 8·202(−3) | 16·1600 | 16·1700 |
| 1·980 | 1·397(−3) | 5·042(−4) | 8·343(−3) | 15·9500 | 15·9600 |
| 2·000 | 1·386(−3) | 5·076(−4) | 8·368(−3) | 13·4100 | 13·4200 |
| 2·040 | 1·366(−3) | 5·142(−4) | 8·495(−3) | 7·2910 | 7·3020 |
| 2·050 | 1·361(−3) | 5·158(−4) | 8·527(−3) | 6·0620 | 6·0740 |
| 2·067 | 1·352(−3) | 5·185(−4) | 8·579(−3) | 4·3590 | 4·3700 |
| 2·084 | 1·344(−3) | 5·212(−4) | 8·631(−3) | 3·1130 | 3·1250 |
| 2·100 | 1·337(−3) | 5·236(−4) | 8·679(−3) | 2·3330 | 2·3440 |
| 2·160 | 1·311(−3) | 5·324(−4) | 8·853(−3) | 3·2630 | 3·2740 |
| 2·200 | 1·295(−3) | 5·378(−4) | 8·965(−3) | 9·1920 | 9·2040 |
| 2·300 | 1·260(−3) | 5·502(−4) | 9·227(−3) | 20·0300 | 20·0400 |
| 2·350 | 1·244(−3) | 5·557(−4) | 9·350(−3) | 14·7300 | 14·7400 |
| 2·400 | 1·230(−3) | 5·607(−4) | 9·467(−3) | 8·9970 | 9·0090 |
| 2·410 | 1·227(−3) | 5·617(−4) | 9·490(−3) | 7·8820 | 7·8940 |
| 2·415 | 1·226(−3) | 5·621(−4) | 9·501(−3) | 7·3420 | 7·3540 |
| 2·420 | 1·225(−3) | 5·626(−4) | 9·512(−3) | 6·8210 | 6·8340 |
| 2·423 | 1·224(−3) | 5·629(−4) | 9·519(−3) | 6·5210 | 6·5330 |
| 2·425 | 1·224(−3) | 5·630(−4) | 9·523(−3) | 6·3260 | 6·3380 |
| 2·430 | 1·222(−3) | 5·635(−4) | 9·535(−3) | 5·8640 | 5·8760 |
| 2·450 | 1·217(−3) | 5·653(−4) | 9·579(−3) | 4·5440 | 4·5560 |
| 2·460 | 1·215(−3) | 5·661(−4) | 9·639(−3) | 4·3440 | 4·3570 |
| 2·467 | 1·213(−3) | 5·667(−4) | 9·616(−3) | 4·4330 | 4·4460 |
| 2·484 | 1·209(−3) | 5·681(−4) | 9·652(−3) | 5·4340 | 5·4470 |
| 2·487 | 1·209(−3) | 5·684(−4) | 9·658(−3) | 5·7120 | 5·7240 |

**Table 3. Partial vibrationally inelastic 0 → 1 cross sections (in $a_0^2$)—continued**

| $E$ (eV) | $\Sigma_g$ | $\Sigma_u$ | $\Pi_u$ | $\Pi_g$ | Total |
|---|---|---|---|---|---|
| 2·490 | 1·208(−3) | 5·686(−4) | 9·665(−3) | 6·0130 | 6·0250 |
| 2·494 | 1·207(−3) | 5·689(−4) | 9·673(−3) | 6·4460 | 6·4580 |
| 2·495 | 1·207(−3) | 5·690(−4) | 9·675(−3) | 6·5590 | 6·5720 |
| 2·500 | 1·206(−3) | 5·694(−4) | 9·686(−3) | 7·1470 | 7·1600 |
| 2·600 | 1·186(−3) | 5·763(−4) | 9·885(−3) | 15·9700 | 15·9800 |
| 2·700 | 1·171(−3) | 5·815(−4) | 1·007(−2) | 12·8700 | 12·8800 |
| 2·733 | 1·167(−3) | 5·828(−4) | 1·012(−2) | 8·5780 | 8·5910 |
| 2·766 | 1·164(−3) | 5·839(−4) | 1·018(−2) | 5·1520 | 5·1650 |
| 2·770 | 1·163(−3) | 5·840(−4) | 1·018(−2) | 4·8820 | 4·8950 |
| 2·800 | 1·160(−3) | 5·849(−4) | 1·023(−2) | 3·9120 | 3·9250 |
| 2·850 | 1·156(−3) | 5·860(−4) | 1·031(−2) | 5·2880 | 5·3010 |
| 2·860 | 1·156(−3) | 5·862(−4) | 1·032(−2) | 5·8300 | 5·8430 |
| 2·900 | 1·153(−3) | 5·867(−4) | 1·038(−2) | 8·4490 | 8·4620 |
| 2·925 | 1·152(−3) | 5·869(−4) | 1·042(−2) | 10·2500 | 10·2600 |
| 2·950 | 1·151(−3) | 5·871(−4) | 1·045(−2) | 11·9200 | 11·9300 |
| 3·000 | 1·149(−3) | 5·871(−4) | 1·051(−2) | 13·5600 | 13·5800 |
| 3·033 | 1·149(−3) | 5·869(−4) | 1·056(−2) | 12·4800 | 12·4900 |
| 3·066 | 1·148(−3) | 5·865(−4) | 1·060(−2) | 9·9290 | 9·9420 |
| 3·100 | 1·148(−3) | 5·860(−4) | 1·064(−2) | 6·9840 | 6·9980 |
| 3·115 | 1·148(−3) | 5·857(−4) | 1·065(−2) | 5·8660 | 5·8800 |
| 3·200 | 1·150(−3) | 5·836(−4) | 1·074(−2) | 3·0490 | 3·0620 |
| 3·250 | 1·152(−3) | 5·820(−4) | 1·079(−2) | 3·7370 | 3·7500 |
| 3·300 | 1·154(−3) | 5·801(−4) | 1·084(−2) | 5·3620 | 5·3760 |
| 3·340 | 1·157(−3) | 5·784(−4) | 1·088(−2) | 6·5610 | 6·5750 |
| 3·350 | 1·157(−3) | 5·780(−4) | 1·089(−2) | 6·7480 | 6·7620 |
| 3·400 | 1·161(−3) | 5·756(−4) | 1·093(−2) | 6·6880 | 6·7020 |
| 3·420 | 1·162(−3) | 5·746(−4) | 1·094(−2) | 6·2500 | 6·2640 |
| 3·450 | 1·165(−3) | 5·730(−4) | 1·097(−2) | 5·3620 | 5·3760 |
| 3·500 | 1·169(−3) | 5·702(−4) | 1·101(−2) | 3·8430 | 3·8570 |
| 3·550 | 1·174(−3) | 5·673(−4) | 1·104(−2) | 2·7800 | 2·7940 |
| 3·600 | 1·179(−3) | 5·641(−4) | 1·107(−2) | 2·3350 | 2·3490 |
| 3·650 | 1·185(−3) | 5·608(−4) | 1·110(−2) | 2·4440 | 2·4580 |
| 3·700 | 1·191(−3) | 5·574(−4) | 1·113(−2) | 2·8610 | 2·8760 |
| 3·750 | 1·197(−3) | 5·539(−4) | 1·116(−2) | 3·1910 | 3·2050 |
| 3·800 | 1·204(−3) | 5·502(−4) | 1·118(−2) | 3·1680 | 3·1830 |
| 3·900 | 1·218(−3) | 5·427(−4) | 1·123(−2) | 2·4040 | 2·4180 |
| 4·000 | 1·233(−3) | 5·351(−4) | 1·127(−2) | 1·7130 | 1·7280 |
| 4·200 | 1·265(−3) | 5·197(−4) | 1·132(−2) | 1·4550 | 1·4700 |
| 4·500 | 1·317(−3) | 4·984(−4) | 1·137(−2) | 0·8902 | 0·9050 |
| 5·000 | 1·406(−3) | 4·740(−4) | 1·136(−2) | 0·5064 | 0·5215 |
| 6·000 | 1·580(−3) | 4·977(−4) | 1·115(−2) | 0·1972 | 0·2127 |
| 7·000 | 1·750(−3) | 6·467(−4) | 1·081(−2) | 0·1043 | 0·1201 |
| 8·000 | 1·944(−3) | 9·410(−4) | 1·044(−2) | 0·0648 | 0·0809 |
| 9·000 | 2·184(−3) | 1·412(−3) | 1·010(−2) | 0·0440 | 0·0609 |
| 10·00 | 2·477(−3) | 2·126(−3) | 9·838(−3) | 0·0317 | 0·0496 |

**Table 4. Theoretical MERT/VCC momentum transfer cross sections (in $a_0^2$) for vibrational transitions $v_0 = 0 \rightarrow v = 0$, 1, 2 and 3**

The final column shows the sum of these, the grand total momentum transfer cross section

| $E$ (eV) | $0 \rightarrow 0$ | $0 \rightarrow 1$ | $0 \rightarrow 2$ | Total |
|---|---|---|---|---|
| 0·020 | 10·659 | 0·000 | 0·000 | 10·659 |
| 0·040 | 14·212 | 0·000 | 0·000 | 14·212 |
| 0·060 | 16·921 | 0·000 | 0·000 | 16·921 |
| 0·080 | 19·165 | 0·000 | 0·000 | 19·165 |
| 0·100 | 21·074 | 0·000 | 0·000 | 21·074 |
| 0·120 | 22·727 | 0·000 | 0·000 | 22·727 |
| 0·140 | 24·180 | 0·000 | 0·000 | 24·180 |
| 0·160 | 25·471 | 0·000 | 0·000 | 25·471 |
| 0·180 | 26·626 | 0·000 | 0·000 | 26·626 |
| 0·200 | 27·664 | 0·000 | 0·000 | 27·664 |
| 0·230 | 29·033 | 0·000 | 0·000 | 29·033 |
| 0·260 | 30·212 | 0·000 | 0·000 | 30·212 |
| 0·290 | 31·234 | 0·001 | 0·000 | 31·236 |
| 0·320 | 32·126 | 0·004 | 0·000 | 32·130 |
| 0·350 | 32·904 | 0·005 | 0·000 | 32·909 |
| 0·550 | 36·089 | 0·007 | 0·000 | 36·095 |
| 0·700 | 37·119 | 0·007 | 0·000 | 37·126 |
| 0·800 | 37·467 | 0·009 | 0·000 | 37·475 |
| 1·000 | 37·759 | 0·014 | 0·000 | 37·773 |
| 1·250 | 38·045 | 0·042 | 0·001 | 38·089 |
| 1·330 | 38·272 | 0·066 | 0·003 | 38·341 |
| 1·361 | 38·395 | 0·079 | 0·004 | 38·478 |
| 1·500 | 39·369 | 0·199 | 0·015 | 39·583 |
| 1·600 | 40·764 | 0·420 | 0·044 | 41·229 |
| 1·700 | 43·375 | 0·989 | 0·149 | 44·514 |
| 1·750 | 45·530 | 1·612 | 0·297 | 47·440 |
| 1·800 | 48·671 | 2·781 | 0·636 | 52·088 |
| 1·850 | 53·277 | 5·139 | 1·492 | 59·907 |
| 1·900 | 59·069 | 9·942 | 3·793 | 72·804 |
| 1·950 | 59·686 | 16·190 | 8·556 | 84·431 |
| 1·980 | 53·408 | 15·948 | 10·646 | 80·002 |
| 2·000 | 48·758 | 13·396 | 10·680 | 72·834 |
| 2·040 | 45·091 | 7·272 | 8·882 | 61·245 |
| 2·050 | 45·439 | 6·045 | 8·360 | 59·843 |
| 2·067 | 46·951 | 4·345 | 7·536 | 58·832 |
| 2·084 | 49·466 | 3·104 | 6·811 | 59·381 |
| 2·100 | 52·661 | 2·329 | 6·210 | 61·200 |
| 2·160 | 71·405 | 3·276 | 4·175 | 78·856 |
| 2·200 | 85·289 | 9·206 | 2·473 | 96·968 |
| 2·300 | 53·233 | 19·975 | 2·777 | 75·984 |
| 2·350 | 45·682 | 14·674 | 6·135 | 66·491 |
| 2·400 | 57·477 | 8·953 | 10·595 | 77·025 |
| 2·410 | 62·017 | 7·842 | 11·567 | 81·426 |
| 2·415 | 64·518 | 7·304 | 12·039 | 83·860 |

**Table 4. Theoretical momentum transfer cross sections (in $a_0^2$)—continued**

| $E$ (eV) | $0 \rightarrow 0$ | $0 \rightarrow 1$ | $0 \rightarrow 2$ | Total |
|---|---|---|---|---|
| 2·420 | 67·143 | 6·785 | 12·491 | 86·419 |
| 2·423 | 68·766 | 6·485 | 12·749 | 88·000 |
| 2·425 | 69·863 | 6·291 | 12·913 | 89·068 |
| 2·430 | 72·638 | 5·831 | 13·295 | 91·764 |
| 2·450 | 83·156 | 4·517 | 14·155 | 101·828 |
| 2·460 | 87·074 | 4·319 | 14·006 | 105·399 |
| 2·467 | 88·858 | 4·409 | 13·623 | 106·889 |
| 2·484 | 89·088 | 5·409 | 11·786 | 106·283 |
| 2·487 | 88·514 | 5·686 | 11·354 | 105·554 |
| 2·490 | 87·772 | 5·986 | 10·901 | 104·658 |
| 2·494 | 86·541 | 6·418 | 10·268 | 103·226 |
| 2·495 | 86·193 | 6·531 | 10·106 | 102·829 |
| 2·500 | 84·244 | 7·117 | 9·282 | 100·643 |
| 2·600 | 46·619 | 15·906 | 0·958 | 63·483 |
| 2·700 | 66·376 | 12·821 | 8·206 | 87·403 |
| 2·733 | 74·656 | 8·546 | 10·784 | 93·986 |
| 2·766 | 74·337 | 5·130 | 11·065 | 90·532 |
| 2·770 | 73·761 | 4·860 | 10·953 | 89·574 |
| 2·800 | 67·431 | 3·890 | 9·518 | 80·839 |
| 2·850 | 55·669 | 5·258 | 6·456 | 67·382 |
| 2·860 | 53·736 | 5·798 | 5·886 | 65·419 |
| 2·900 | 48·143 | 8·409 | 3·885 | 60·436 |
| 2·925 | 46·568 | 10·202 | 2·875 | 59·645 |
| 2·950 | 46·594 | 11·872 | 2·078 | 60·543 |
| 3·000 | 50·980 | 13·524 | 1·340 | 65·844 |
| 3·033 | 55·088 | 12·452 | 1·598 | 69·138 |
| 3·066 | 57·610 | 9·916 | 2·268 | 69·794 |
| 3·100 | 57·537 | 6·981 | 3·030 | 67·548 |
| 3·115 | 56·792 | 5·865 | 3·318 | 65·975 |
| 3·200 | 49·753 | 3·046 | 4·135 | 56·933 |
| 3·250 | 46·350 | 3·727 | 4·033 | 54·111 |
| 3·300 | 44·811 | 5·350 | 3·467 | 53·628 |
| 3·340 | 45·046 | 6·552 | 2·694 | 54·292 |
| 3·350 | 45·249 | 6·741 | 2·477 | 54·467 |
| 3·400 | 46·351 | 6·691 | 1·491 | 54·533 |
| 3·420 | 46·572 | 6·257 | 1·219 | 54·049 |
| 3·450 | 46·508 | 5·374 | 0·986 | 52·868 |
| 3·500 | 45·529 | 3·858 | 0·981 | 50·368 |
| 3·600 | 42·562 | 2·348 | 1·617 | 46·527 |
| 3·700 | 40·952 | 2·873 | 1·904 | 45·730 |
| 3·800 | 40·808 | 3·187 | 1·189 | 45·184 |
| 4·000 | 39·018 | 1·737 | 0·474 | 41·228 |
| 5·000 | 34·165 | 0·531 | 0·105 | 34·801 |
| 6·000 | 32·434 | 0·217 | 0·023 | 32·674 |
| 7·000 | 31·616 | 0·121 | 0·009 | 31·746 |
| 8·000 | 31·116 | 0·080 | 0·004 | 31·201 |
| 9·000 | 30·739 | 0·059 | 0·003 | 30·801 |
| 10·000 | 30·415 | 0·047 | 0·002 | 30·463 |

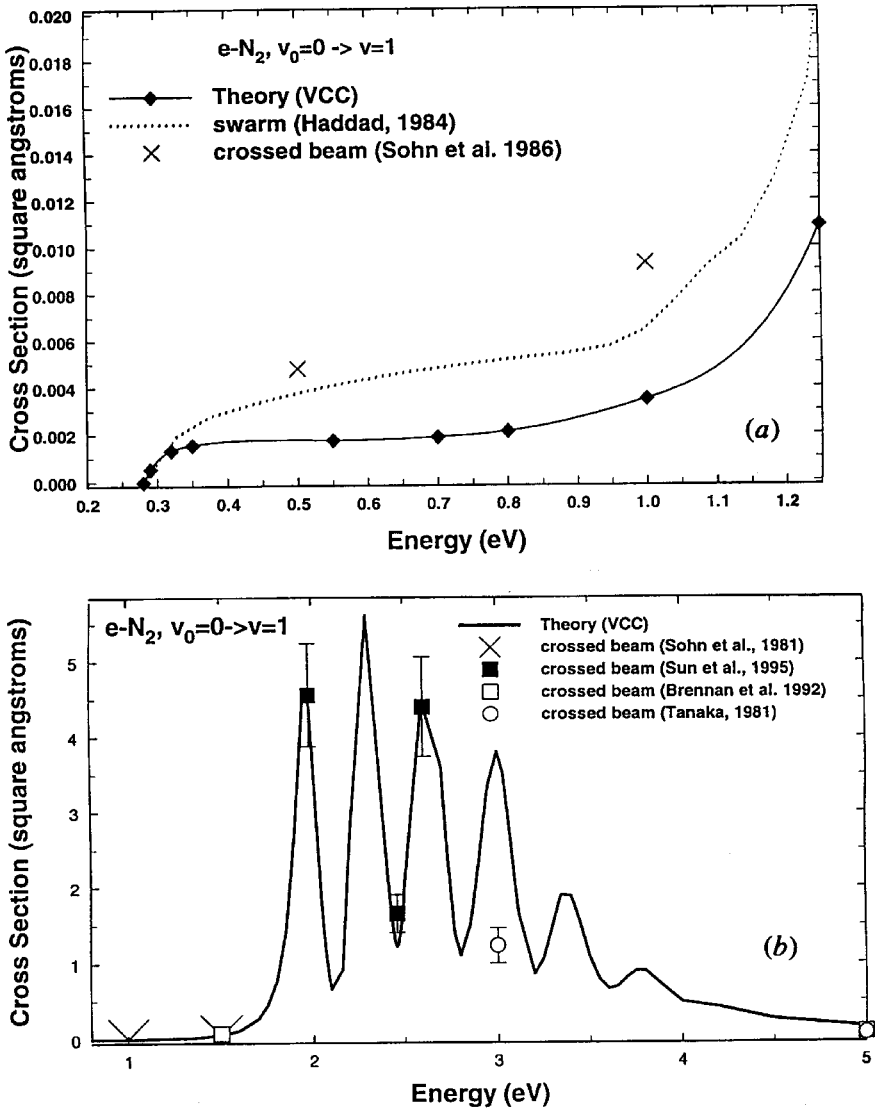


**Fig. 8.** Cross sections for the $v_0 = 0 \rightarrow v = 1$ vibrational excitation of $N_2$ as functions of electron energy as calculated using the VCC theory of Morrison *et al.* (1996) (solid curve with diamonds) at energies (*a*) below the 2·4 eV shape resonance and (*b*) in the resonance region. Also shown in (*a*) are the swarm-derived values of Haddad (1984) (dotted curve) and in (*a*) and (*b*) the crossed-beam data of Sohn *et al.* (1986) (crosses).

vibrational cross section; they also found that its magnitude had to be similar to Chen's prediction. In his subsequent analysis of transport data in nitrogen–argon mixtures in order to reexamine vibrational excitation in the resonance region, Haddad (1984) used the cross section of Engelhardt *et al.* below the resonance. In the present study we have tested both this cross section and the theoretical cross sections of Sun *et al.* (1995) for compatibility with the present drift velocity data for the nitrogen–neon mixture.

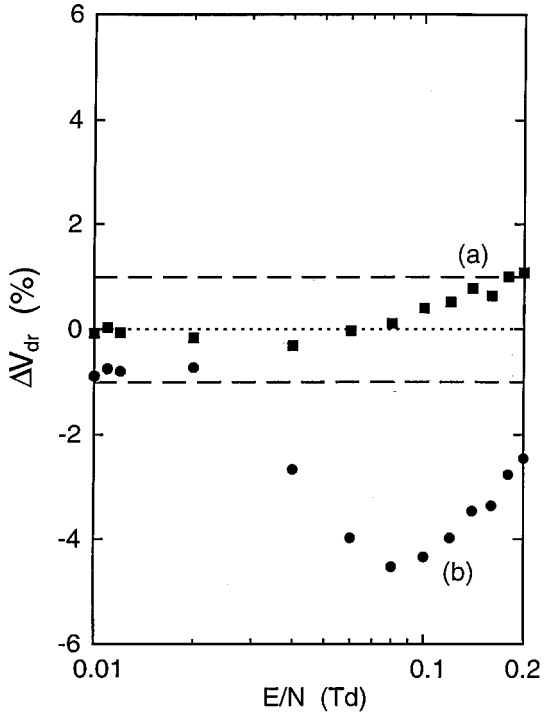


**Fig. 9.** The differences (%), as functions of $E/N$, between the measured drift velocities for a 2·085% $N_2$–97·915% Ne mixture at 76·8 K and those calculated with different sets of cross sections for momentum transfer, rotational, and vibrational excitation (see Section 7): (a) set 1; (b) set 2. For Ne the momentum transfer cross section of Robertson (1972) and O'Malley and Crompton (1980) was used in all calculations, and for $N_2$ that of Morrison *et al.* (1996).

Energy loss through vibrational excitation begins to influence the electron energy distribution functions and hence the drift velocities above 0·012 Td. We have therefore used the data between 0·012 Td and 0·2 Td, the upper limit of our measurements.

**Set 1**

The first set of cross sections tested was that of Haddad (1984). His rotational cross sections were generated with the QBA formula (1) using a vibrationally averaged quadrupole moment $\overline{Q} = -1{\cdot}06\, ea_0^2$. As can be seen from (a) in Fig. 9, this cross section set gives values of $v_{\rm dr}$ which are in agreement with the experimental values over the whole $E/N$ range. Such agreement confirms the earlier conclusions concerning the validity of analyses based on drift and diffusion data in the pure gas (see Section 6).

**Set 2**

The second set consisted of the theoretical MERT/VCC momentum transfer cross section, the VCC vibrational excitation cross sections, and the MERT/VCC

rotational excitation cross sections *multiplied by the factor of 1·3* discussed in the previous section. This calculation included vibrational excitation cross sections $v_0 = 0 \rightarrow v = 1$, 2 and 3, and rotational excitation cross sections $j_0 \rightarrow j_0 + 2$ for $j_0 = 0, 1, 2, \ldots, 12$.

Tests carried out by varying the $v_0 = 0 \rightarrow v = 1$ cross section indicated that the drift velocities measured in these experiments are insensitive to this cross section at energies greater than about 1·0 eV. The $v_0 = 0 \rightarrow v = 2$ and 3 cross sections were found to have only a relatively small effect on the calculated drift velocities; deleting them caused a change in $v_{\mathrm{dr}}$ at 0·2 Td of less than 0·1%. The theoretical momentum transfer cross section is shown in Fig. 6. In the energy range of significance to these calculations there is good agreement between the theoretical cross section and the experimental cross sections derived from several sources which are shown for comparison.

Curve (b) of Fig. 9 shows that the differences between the measured drift velocities and those calculated with this set of cross sections are well outside experimental error. Moreover, the differences have been somewhat reduced because the rotational cross sections have been scaled everywhere by the factor of 1·3, whereas such scaling can only be justified in the non-resonant region, i.e. up to at most 0·5 eV. Tests have shown that the theoretical vibrational cross section would need to be increased by at least 50% in this threshold region to obtain agreement between measured and calculated values.

## 8. Conclusion

This investigation of low-energy electron scattering in nitrogen by new theoretical calculations and the analysis of new drift velocity data for a nitrogen–neon mixture has thrown significant light on e–$N_2$ rotational and vibrational excitation. Although, as will be clear from the discussion in Section 4, no information about the momentum transfer cross section for nitrogen can be obtained by comparisons with the present drift velocity data in the mixture, the MERT/VCC theory yields an e–$N_2$ momentum transfer cross section in excellent agreement with the cross sections derived from previous swarm analyses and crossed beam studies (see Fig. 6). Such agreement inspires considerable confidence in the assumptions underlying this study and in the numerical precision of the present solution of the Schrödinger equation. This confidence is enhanced by our finding that the theoretical rotational excitation cross sections, after a scaling justified by physical arguments, are in good agreement with the present data. The theoretical study of Morrison *et al.* (1996) has answered the long standing question of why the QBA rotational excitation cross sections, which have a very limited range of validity, led fortuitously to good agreement with the experimental transport coefficient data for nitrogen, and why they also led to equally good agreement with the drift velocity data for the nitrogen–neon mixture used in the present study. It is, therefore, surprising and disappointing that the theoretical vibrational excitation cross sections at energies up to about 1 eV are not compatible with the present drift velocity data. We note in conclusion that the differences between $v_0 = 0 \rightarrow v = 1$ vibrational cross sections derived from theory and experiment for e–$H_2$ scattering at energies below about 1·5 eV, about which much has been written (see Morrison *et al.* 1987*a*; Buckman *et al.* 1990; Crompton and Morrison 1993), is of comparable magnitude to that in e–$N_2$ scattering *but of the opposite*

*sign*. These at present unexplained serious disparities between vibrational cross sections from theoretical calculations and from transport analysis demand further investigation.

**Acknowledgments**

We would like to acknowledge useful discussions with Dr Stephen Buckman concerning various aspects of this research. MAM gratefully acknowledges the hospitality of the Australian National University, where this paper was completed, the Fulbright Commission (Australian–American Educational Foundation) for a Senior Scholar Grant to Australia during 1996, and the support of the National Science Foundation under Grant No. PHY–9408977.

**References**

Brennan, M. J., Alle, D. T., Euripides, P., Buckman, S. J., and Brunger, M. J. (1992). *J. Phys*. B **25**, 2669.
Bridge, N. J., and Buckingham, A. D. (1966). *Proc. R. Soc. London* A **295**, 334.
Buckman, S. J. (1995). personal communication.
Buckman, S. J., Brunger, M. J., Newman, D. S., Snitchler, G., Alston S., Norcross, D. W., Morrison, M. A., Saha, B. C., Danby G., and Trail, W. K. (1990). *Phys. Rev. Lett.* **65**, 3253.
Chang, E. S., and Fano, U. (1972). *Phys. Rev.* A **6**, 173.
Chang, E. S., and Temkin, A. (1969). *Phys. Rev. Lett.* **23**, 399.
Chen, J. C. Y. (1964). *J. Chem. Phys.* **40**, 3513.
Crompton, R. W. (1989). *In* 'Nonequilibrium Effects in Ion and Electron Transport' (Eds J. W. Gallagher *et al.*), p. 11 (Plenum: New York).
Crompton, R. W., and Morrison, M. A. (1993). *Aust. J. Phys.* **46**, 203.
Dalgarno, A., and Moffett, R. J. (1963). *Proc. Nat. Acad. Sci. India* A **33**, 511.
Engelhardt, A. G., Phelps, A. V., and Risk, C. G. (1964). *Phys. Rev.* **135**, A1566.
England, J. P., and Elford, M. T. (1988). *Aust. J. Phys.* **41**, 701.
England, J. P., and Elford, M. T. (1991). *Aust. J. Phys.* **44**, 647.
England, J. P., Elford, M. T., and Crompton, R. W. (1988). *Aust. J. Phys.* **41**, 573.
England, J. P., and Skullerud, H. R. (1997). *Aust. J. Phys.* **50**, 553 (present issue).
Fabrikant, I. I. (1984). *J. Phys.* B **17**, 4223.
Feldt, A. N., and Morrison, M. A. (1984). *Phys. Rev.* A **29**, 401.
Frost, L. S., and Phelps, A. V. (1962). *Phys. Rev.* **127**, 1621.
Gerjuoy, E., and Stein, S. (1955). *Phys. Rev.* **97**, 1671; **98**, 1848.
Gibson, D. K. (1970). *Aust. J. Phys.* **23**, 683.
Gibson, T. L., and Morrison, M. A. (1981). *J. Phys.* B **14**, 727.
Gibson, T. L., and Morrison, M. A. (1982). *J. Phys.* B **15**, L221.
Gibson, T. L., and Morrison, M. A. (1984). *Phys. Rev.* A **29**, 2497.
Gulley, R. J., Alle, D. T., Brennan, M. J., and Buckman, S. J. (1994). *J. Phys.* B **27**, 2593.
Haddad, G. N. (1983). *Aust. J. Phys.* **36**, 297.
Haddad, G. N. (1984). *Aust. J. Phys.* **37**, 487.
Haddad, G. N., and Crompton, R. W. (1980). *Aust. J. Phys.* **33**, 975.
Hara, S. (1967). *J. Phys. Soc. Jpn* **22**, 710.
Hara, S. (1969). *J. Phys. Soc. Jpn* **27**, 1592.
Henry, R. J. W. (1970). *Phys. Rev.* **2**, 1349.
Huber, K. P., and Herzberg, G. (1979). 'Molecular Spectra and Molecular Structure IV. Constants of Diatomic Molecules' (Van Nostrand: New York).
Huxley, L. G. H., and Crompton, R. W. (1974). 'The Diffusion and Drift of Electrons in Gases' (Wiley–Interscience: New York).
Isaacs, W. A., and Morrison, M. A. (1992). *J. Phys.* B **25**, 703.

Isaacs, W. A., and Morrison, M. A. (1996). *Phys. Rev.* A **53**, 4215.
Lane, N. F. (1980). *Rev. Mod. Phys.* **52**, 29.
Lane, N. F., and Henry, R. J. W. (1968). *Phys. Rev.* **173**, 183.
Mason, E. A., and McDaniel E. W. (1988). 'Transport Properties of Ions in Gases' (Wiley: New York).
Miller, T. M., and Bederson, B. (1978). *Adv. At. Mol. Phys.* **13**, 1.
Mjolsness, R. C., and Sampson, D. H. (1964). *Phys. Rev. Lett.* **13**, 812.
Morrison, M. A. (1979). *In* 'Electron– and Photon–Molecule Collisions' (Eds T. N. Rescigno *et al.*), pp. 15–51 (Plenum: New York).
Morrison, M. A. (1983). *Aust. J. Phys.* **36**, 239.
Morrison, M. A. (1988). *Adv. At. Mol. Phys.* **24**, 51.
Morrison, M. A., and Collins, L. A. (1978). *Phys. Rev.* A **17**, 918.
Morrison, M. A., and Collins, L. A. (1981). *Phys. Rev.* A **23**, 127.
Morrison, M. A., Crompton, R. W., Saha, B. C., and Petrović, Z. Lj. (1987*a*). *Aust. J. Phys.* **40**, 239.
Morrison, M. A., Feldt A. N., and Austin, D. (1984*a*). *Phys. Rev.* A **29**, 2518.
Morrison, M. A., Feldt, A. N., and Saha, B. C. (1984*b*). *Phys. Rev.* A **30**, 2811.
Morrison, M. A., and Saha, B. C. (1986). *Phys. Rev.* A **34**, 2786.
Morrison, M. A., Saha, B. C., and Gibson, T. L. (1987*b*). *Phys. Rev.* A **36**, 3682.
Morrison, M. A., and Sun, W. (1995). *In* 'Computation Methods of Electron–Molecule Scattering Theory' (Eds W. Huo and F. A. Gianturco), pp. 131–190 (Plenum: New York).
Morrison, M. A., Sun, W., Isaacs, W. A., and Trail, W. K. (1997). *Phys. Rev.* A **55**, 278.
Morrison, M. A., and Trail, W. K. (1993). *Phys. Rev.* **48**, 2874.
Newell, A. C., and Baird, R. C. (1965). *J. Appl. Phys.* **36**, 3751.
O'Malley, T. F., and Crompton, R. W. (1980). *J. Phys.* B **13**, 3451.
Onda, K. (1985). *J. Phys. Soc. Jpn* **54**, 4544.
Orcutt, R. H., and Cole, R. H. (1967). *J. Chem. Phys.* **46**, 697.
Petrović, Z. Lj., and Crompton, R. W. (1987). *Aust. J. Phys.* **40**, 347.
Phelps, A. V., and Pitchford, L. C. (1985). *Phys. Rev.* A **31**, 2932.
Robertson, A. G. (1972). *J. Phys.* B **5**, 648.
Saha, H. P. (1990). *Phys. Rev. Lett.* **65**, 2003.
Sampson, D. H., and Mjolsness, R. C. (1965). *Phys. Rev.* **140**, A1466.
Sams, W. N. , and Kouri, D. J. (1969). *J. Chem. Phys.* **51**, 4809.
Schmidt, B. (1995). personal communication.
Schmidt, B., Berkhan, K. G., Fitz, B., and Fuller, M. (1994). *Phys. Scripta* T **53**, 30.
Schulz, G. J. (1964). *Phys. Rev.* **135**, A988.
Shyn, T. W., and Carignan, G. R. (1980). *Phys. Rev.* A **22**, 923.
Sohn, W., Kochem, K.-H., Scheuerlein, K.-M., Jung, K., and Ehrhardt, H. (1986). *J. Phys.* B **19**, 4017.
Sun, W., Morrison, M. A., Isaacs, W. A., Trail, W. K., Alle, D. T., Gulley R. J., Brennan, M. J., and Buckman, S. J. (1995). *Phys. Rev.* A **52**, 1229.
Tachibana, K., and Phelps, A. V. (1979). *J. Chem. Phys.* **71**, 3544.
Temkin, A. (1957). *Phys. Rev.* **107**, 1004.
Temkin, A., and Vasavada, K. V. (1967). *Phys. Rev.* A **160**, 190.
Townsend, J. S., and Bailey, V. A. (1922). *Phil. Mag.* **44**, 1033.
Trail, W. K. (1992). PhD thesis, University of Oklahoma.
Trail, W. K., and Morrison, M. A. (1996). (in preparation).
Weatherford, C., and Temkin, A. (1994). *Phys. Rev.* A **49**, 2580.

## Appendix: Weighting of the Rotational Excitation Cross Sections

The fractional populations, $f_j$, of the rotational states $j$ of the nitrogen molecule in a gas of such molecules at absolute temperature $T$ are given by

$$f_j = \frac{p_j}{P_r}\, e^{-e\epsilon_j/(k_B T)}\,, \tag{1}$$

where $\epsilon_j$ is the energy of the $j^{\text{th}}$ rotational state and $k_B$ is Boltzmann's constant. The statistical weight factor $p_j/P_r$ is given by the ratio of

$$p_j = (2t+1)(t+a)(2j+1) = 3(1+a)(2j+1)\,, \tag{2a}$$

$$P_r = \sum_j p_j e^{-e\epsilon_j/(k_B T)}\,, \tag{2b}$$

where $t$ is the nuclear spin of the atom ($t = 1$ for nitrogen) and the coefficient $a = 0$ for odd $j$ and $a = 1$ for even $j$. The energy levels $\epsilon_j$ for the nitrogen molecule in its ground vibrational state (relative to the energy of the $j = 0$ state) were calculated from the expression and constants given by Huber and Herzberg (1979).

Each cross section for a specific excitation $j_0 \to j$ was weighted first by the fractional abundance $f_j$ of the lower state and second by the mixture fraction $0{\cdot}02885$. Only transitions involving $\Delta j = \pm 2$ were included; for $E_0 < 1{\cdot}5$ eV rotational transitions for $\Delta j \geq 2$ make negligible contributions to energy exchange.

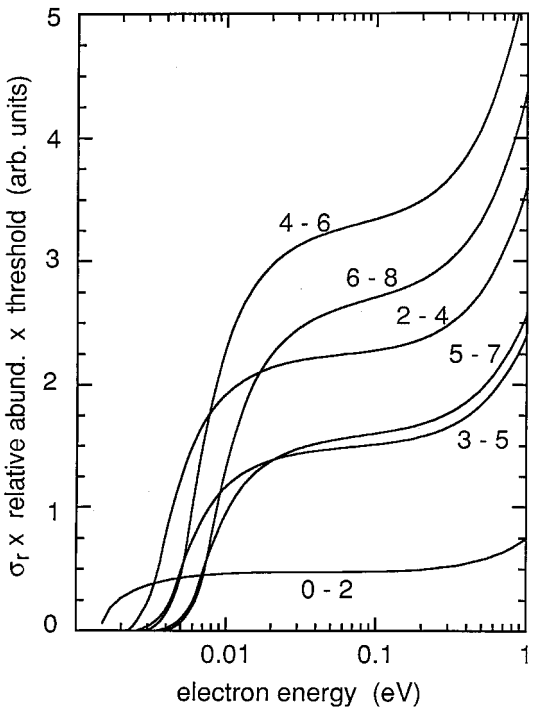


**Fig. 10.** The weighted rotational excitation cross sections of Morrison *et al.* (1996) as functions of electron energy. The $j_0 = 1 \to j = 3$ cross section and those with thresholds higher than $j_0 = 6$ have been omitted. The cross sections have been weighted by the relative abundance of the $j_0$ level for a gas temperature of $76{\cdot}8$ K and by the associated energy loss in order to demonstrate the significance of particular rotational excitations in determining the rate of energy transfer by electrons at a given energy.

The QBA cross sections can be easily calculated for any particular rotational transition. However, in more accurate calculations such as those of Morrison *et al.* (1996)—where the vibrational dynamics are fully taken into account and the interaction potential includes terms representing static, exchange, polarisation, and bound–free correlation effects—generating the many rotational excitation cross sections required for calculation of the drift velocity could entail an excessive amount of computation. Hence Trail and Morrison (1996) have developed and implemented scaling relations to generate the required rotational cross sections.

In order to check the reliability of these relations, we compared $\sigma^{(r)}_{1\to 3}(E_0)$ (threshold, $2{\cdot}48$ meV) as calculated directly from the BFVCC scattering matrix by Morrison *et al.* (1996) to the same cross section as generated by scaling their theoretical $j_0 = 0 \to j = 2$ cross section. At energies between 3 and 80 meV, the $j_0 = 1 \to j = 3$ cross section that resulted from scaling was found to be about 3% lower than the directly calculated theoretical cross sections. As explained in Trail and Morrison (1996), the accuracy of the $j'_0 \to j'$ cross section generated from the scaling relations improves with increasing value of the initial quantum number $j_0$ of the 'base cross section' $\sigma^{(r)}_{j_0\to j}(E_0)$.

The contribution of a specific rotational excitation to the rate of energy exchange depends strongly on the initial quantum number $j_0$. To demonstrate the significance of specific transitions, the theoretical rotational cross sections of Morrison *et al.* were multiplied by the corresponding energy loss for the transition and by the fractional abundances of the initial state. As shown in Fig. 10, the most significant energy loss processes under the experimental conditions of the present study are those for which $j_0$ is 2, 4 and 6. By contrast, excitations from the $j_0 = 0$ and $j = 1$ states contribute very little to rotational energy exchange, due to their low threshold energies and the small populations of these initial states at $76{\cdot}8$ K. (For example, for the $j_0 = 0 \to j = 2$ transition, $\epsilon_0 = 1{\cdot}488$ meV and $f_0 = 0{\cdot}0493$.)

Manuscript received 19 August 1996, accepted 23 January 1997